
CONTINUOUS TIME LOCALLY STATIONARY WAVELET PROCESSES

Henry Antonio Palasciano

Department of Mathematics
Imperial College London
SW7 2AZ, London, UK

henry.palasciano17@imperial.ac.uk

Marina I. Knight

Department of Mathematics
University of York
YO10 5DD, York, UK

marina.knight@york.ac.uk

Guy P. Nason

Department of Mathematics
Imperial College London
SW7 2AZ, London, UK

g.nason@imperial.ac.uk

May 20, 2024

ABSTRACT

This article introduces the class of continuous time locally stationary wavelet processes. Continuous time models enable us to properly provide scale-based time series models for irregularly-spaced observations for the first time, while also permitting a spectral representation of the process over a continuous range of scales. We derive results for both the theoretical setting, where we assume access to the entire process sample path, and a more practical one, which develops methods for estimating the quantities of interest from sampled time series. The latter estimates are accurately computable in reasonable time by solving the relevant linear integral equation using the iterative thresholding method due to Daubechies, Defrise and De Mol. Appropriate smoothing techniques are also developed and applied in this new setting. We exemplify our new methods by computing spectral and autocovariance estimates on irregularly-spaced heart rate data obtained from a recent sleep-state study.

Keywords Continuous time models, Irregular spacing, Local autocovariance, Non-stationary time series, Wavelets, Wavelet spectrum

1 Introduction

It is often customary to assume that a time series is (second-order) stationary, since, in this case, plenty of theoretically sound and well-tested methods are readily available for its analysis, see, e.g., [1] or [2]. However, in practice, many time series are unlikely to be stationary. For example, many financial time series are often non-stationary [3, 4, 5, 6]. It is well known that a stationary stochastic process $X(t)$, $t \in \mathbb{R}$, has a spectral representation of the form

$$X(t) = \int_{-\infty}^{\infty} \exp(i\omega t) dZ(\omega), \quad (1)$$

where $Z(\omega)$ is a square-integrable orthogonal increment process satisfying $\mathbb{E}[|dZ(\omega)|^2] = dS^{(I)}(\omega)$ and $S^{(I)}(\omega)$ is the integrated spectrum of $X(t)$. The autocovariance function of $X(t)$, $c(\tau)$, has a similar representation in the frequency domain,

$$c(\tau) = \int_{-\infty}^{\infty} \exp(i\omega\tau) dS^{(I)}(\omega), \quad (2)$$

see, e.g., [7]. To extend these quantities to the non-stationary case, [7] suggested introducing a time-varying amplitude function $A(t, \omega)$ into (1) giving

$$X(t) = \int_{-\infty}^{\infty} A(t, \omega) \exp(i\omega t) dZ(\omega). \quad (3)$$

Models such as (3) form the basis for locally stationary time series, later developed by [8] in discrete time.

[9] introduced the locally stationary *wavelet* (LSW) processes, which replaced the set of functions $\{\exp(i\omega t)\}$ with a set of discrete non-decimated wavelets. As with locally stationary Fourier processes [8], the process local stationarity is enforced via constraints on their amplitude functions. From LSW processes, one can then obtain a time-scale decomposition of the spectral density function, known as the evolutionary wavelet spectrum, and a wavelet representation of the local autocovariance similar to (2).

However, discrete time LSW processes are constructed under the assumption that the time series data are obtained at a constant sampling rate, which is not always appropriate as, in practice, observations can either be missing or be irregularly-spaced. Attempts to provide a suitable alternative for irregularly-spaced data were made in [10] and [11] via the use of the lifting transform. Unfortunately: 1. the estimates in [10, 11] only resemble the true quantity defined in [9] in that they can only estimate an underlying spectrum at time points in the irregular sample and nowhere in between; 2. [11] state that their methods are "highly computationally intensive" in that estimation, for each time point, requires the computation of a full lifting (second generation wavelet) transform for multiple, P , simulations corresponding to different trajectories for the lifting algorithm. To get good estimation, typically P is large. In [11] values for P of 1000 and 5000 were used. Hence, [11] requires nP lifting (wavelet) transforms compared to our method which uses one (or certainly at least $o(1)$). On the other hand, our method can achieve accuracy and estimates the spectrum itself (not a simulacrum), but importantly it is massively more computationally efficient than the only alternative. This article proposes the use of continuous time locally stationary wavelet processes instead, which are natural counterparts to the discrete time versions developed in [9]. To our knowledge, our new methods are the only ones that can accurately estimate wavelet spectral properties of an irregularly-sampled process within a reasonable computational time frame.

Aside from the practical advantages that a continuous time model provides, our results are also interesting from a more theoretical perspective. In fact, many discrete time models and methods also possess a continuous time counterpart, see [12], [13], [14] and [15] for example. Recently, [16] adapted locally stationary Fourier processes from the discrete (see [8] or [17]) to the continuous time setting. Since, so far, the theory of LSW processes [9] exists in discrete time only, our objective is to introduce parallel continuous time models, study their theoretical properties and develop a practical means for their estimation and analysis. In doing so, we obtain a representation of the evolutionary wavelet spectrum across a *continuous* range of scales, providing a complete decomposition of the underlying frequencies of the process.

Section 2 reviews relevant background material on locally stationary processes in discrete time, Lévy processes and bases, and useful regularisation methods. Section 3 defines our locally stationary wavelet processes, the associated evolutionary wavelet spectrum and local autocovariance, and related concepts all in continuous time. Section 4 demonstrates how our continuous time models can be fitted to irregularly spaced time series, describes methods to appropriately smooth any estimates and develops associated estimation theory. Finally, Section 5 shows the effectiveness of our methods by computing an estimate of the continuous time evolutionary wavelet spectrum to irregularly-spaced heart rate measurements of a sleeping individual and compares this estimate to the corresponding sleep stage time series. Such comparisons can be used to predict expensive and hard to collect sleep stage series from heart rate series that are cheaper and easier to collect, particularly in the home environment.

2 Background

We briefly review some of the necessary background material beginning with locally stationary wavelet processes in discrete time, followed by Lévy bases and conclude with some useful regularisation methods. A more comprehensive review can be found in Supplementary Materials Section A.

(Discrete) locally stationary wavelet (LSW) processes [9, 18] are time series models that have found applications in various domains, including finance [6], economics [19] alias detection [20, 21], biology [22], gravitational-wave detection [23] and energy [24, 25], to name but a few. They are defined as a sequence of stochastic processes indexed by time and have the following representation in the mean square sense:

$$X_{t,T} = \sum_{j=1}^{\infty} \sum_{k=-\infty}^{\infty} w_{j,k;T} \psi_{j,k-t} \xi_{j,k}, \quad (4)$$

where $\{w_{j,k;T}\}_{j \in \mathbb{N}, k \in \mathbb{Z}}$ is a set of amplitudes, $\{\psi_{j,k-t}\}_{j \in \mathbb{N}, k \in \mathbb{Z}}$ are discrete wavelets and $\{\xi_{j,k}\}_{j \in \mathbb{N}, k \in \mathbb{Z}}$ is a set of random variables with zero mean and unit variance. Conditions are also imposed on the amplitude functions to prevent them from varying too quickly, thus preserving the local stationarity of the process. More importantly, one assumes that, as $T \rightarrow \infty$, $w_{j,k;T}$ converges to $W_j(k/T)$, a rescaled time Lipschitz continuous amplitude function defined on $z = k/T \in (0, 1)$, which is known as rescaled time (introduced by [8]) and which is commonly employed when working with locally stationary processes. One can then also define the evolutionary wavelet spectrum of the LSW process by

$$S_j(z) = |W_j(z)|^2 \quad (5)$$

and the autocorrelation wavelets and local autocovariance by

$$\Psi_j(\tau) = \sum_k \psi_{j,k} \psi_{j,k-\tau}, \quad \text{and} \quad c(z, \tau) = \sum_{j=1}^{\infty} S_j(z) \Psi_j(\tau), \quad (6)$$

respectively, where $j \in \mathbb{N}$ and $\tau \in \mathbb{Z}$. To estimate the spectrum, one can use the non-decimated discrete wavelet transform to compute the raw wavelet periodogram and then correct this using an inner product operator. For more details see [9].

Lévy processes and bases play a crucial role in the definition of locally stationary wavelet processes in continuous time. Our discussion draws heavily from [26, 27, 28, 29, 30]. In the following, take $(\Omega, \mathcal{F}, \mathbb{P})$ to be the underlying probability space, $(S, \mathcal{B}(S))$ to be a Borel space and denote the bounded Borel sets of $\mathcal{B}(S)$ by $\mathcal{B}_b(S)$. A real valued Lévy basis on S is a collection $\{L(A) : A \in \mathcal{B}_b(S)\}$ of random variables satisfying the following properties:

- (a) If A and B are disjoint subsets in $\mathcal{B}_b(S)$, then $L(A \cup B) = L(A) + L(B)$, almost surely.
- (b) If A and B are disjoint subsets in $\mathcal{B}_b(S)$, then $L(A)$ and $L(B)$ are independent,
- (c) The law of $L(A)$ is infinitely divisible for all $A \in \mathcal{B}_b(S)$.

Since the law of $L(A)$ is infinitely divisible for all $A \in \mathcal{B}_b(S)$, it has a Lévy-Khintchine representation. We restrict our attention to homogeneous Lévy bases, which is synonymous with the concept of stationarity, as defined by [26]. A homogeneous Gaussian Lévy basis G , for example, is defined as $G(A) \sim \mathcal{N}\{\mu \text{Leb}(A), \sigma^2 \text{Leb}(A)\}$ for all $A \in \mathcal{B}(\mathbb{R}^n)$ and some $\mu \in \mathbb{R}$ and $\sigma \in \mathbb{R}^+$, where Leb denotes the Lebesgue measure. It is equivalent to the concept of white noise as defined in [29]. Furthermore, if L is a homogeneous Lévy basis on $(\mathbb{R}, \mathcal{B}(\mathbb{R}))$, then the process $(L_t)_{t \geq 0}$ with $L_t = L([0, t])$ is a Lévy process and, conversely, given a Lévy process $(L_t)_{t \geq 0}$, we can obtain a Lévy basis L by setting $L((s, t]) = L_t - L_s$.

Linear integral equations, the methods to solve them and regularisation methods for solving linear inverse problems are used here for computing evolutionary wavelet spectral estimates. We summarise key ideas from [31, 32, 33, 34]. Linear integral operators are mappings from $L^2(S)$ to $L^2(S)$, where $S \subset \mathbb{R}^n$, of the form

$$(Th)(x) = \int_S K(x, y) h(y) dy, \quad x \in S, \quad (7)$$

where $K : S \times S \mapsto \mathbb{R}$ is a continuous kernel. For our work, Mercer's ([31]) theorem is key, as we work with continuous symmetric non-negative definite kernels. Hence, the kernel K can be expanded in terms of its eigenvalues λ_n and eigenfunctions φ_n of T as

$$K(x, y) = \sum_{n=1}^{\infty} \lambda_n \varphi_n(x) \varphi_n(y), \quad (8)$$

where the convergence is absolute and uniform. Given f and K , Mercer's theorem permits us to obtain a solution h to the linear integral equation $Th = f$ in terms of the eigendecomposition of K . Typically one also encounters noise contamination of the form $f = g + \varepsilon$, where g denotes the true function and ε the noise, and so regularisation methods such as the spectral cut-off [32] should be employed to mitigate its effects.

Alternatively, $Th = f$ can be reformulated as an optimisation problem to minimise $\Delta h = \|Th - f\|^2$. In the presence of noise, several useful regularisation techniques, such as Tikhonov regularisation, are readily available. Here, we find the iterative thresholding algorithm introduced by [33] useful when computing an estimate of the continuous time evolutionary wavelet spectrum from an estimate of the raw wavelet periodogram, see Section 4.1. We minimise

$$\Phi_{\mu, p}(h) = \|Th - f\|^2 + \sum_{\gamma \in \Gamma} \mu_\gamma |\langle h, e_\gamma \rangle|^p, \quad (9)$$

where $\{e_\gamma\}_{\gamma \in \Gamma}$ is an orthogonal basis of $L^2(S)$, $\mu = \{\mu_\gamma\}_{\gamma \in \Gamma}$ is a vector of weights, which act as regularisation parameters, and $1 \leq p \leq 2$. In particular, we are interested in penalising positive and negative coefficients differently for the case $p = 1$. To do so, one would replace each μ_γ with the positive weights $(\mu_\gamma^+, \mu_\gamma^-)$. The solution can be obtained via an iterative scheme given by

$$h^{(n)} = \mathbf{Shrink}_{\mu, 1} \left\{ h^{(n-1)} + T^\dagger (f - Th^{(n-1)}) \right\}, \quad (10)$$

where T^\dagger denotes the adjoint of T ,

$$\mathbf{Shrink}_{\mu, 1}(h) = \sum_{\gamma \in \Gamma} \mathbf{Shrink}_{\mu_\gamma, 1}(\langle h, e_\gamma \rangle) e_\gamma \quad (11)$$

and

$$\mathit{Shrink}_{\mu_\gamma, 1}(x) = \begin{cases} x - \mu_\gamma^+/2, & \text{if } x \geq \mu_\gamma^+/2, \\ 0, & \text{if } -\mu_\gamma^-/2 < x < \mu_\gamma^+/2, \\ x + \mu_\gamma^-/2, & \text{if } x \leq -\mu_\gamma^-/2. \end{cases} \quad (12)$$

We write the Shrink operator in bold to distinguish the case when this is applied to vectors, as in [33]. As shown in [33], (10) converges to the unique minimiser of (9) for arbitrarily chosen $h^0 \in L^2(S)$. In order to guarantee convergence of this algorithm to the true solution as the noise level ε goes to zero, one selects $\boldsymbol{\mu} = \boldsymbol{\mu}(\varepsilon)$ such that

$$\lim_{\varepsilon \rightarrow 0} \boldsymbol{\mu}(\varepsilon) = 0 \quad \text{and} \quad \lim_{\varepsilon \rightarrow 0} \varepsilon^2 / \boldsymbol{\mu}(\varepsilon) = 0. \quad (13)$$

For more details on this iterative algorithm please see [33] or the Supplementary Materials Section A.

3 Locally Stationary Wavelet Processes in Continuous Time: Theory

Our continuous time locally stationary wavelet processes rely on continuous wavelets $\psi \in L^2(\mathbb{R})$ for which we assume that

$$\int_{-\infty}^{\infty} \psi(x) dx = 0 \quad \text{and} \quad \|\psi\|^2 = \int_{-\infty}^{\infty} |\psi(x)|^2 dx = 1. \quad (14)$$

From $\psi \in L^2(\mathbb{R})$ an entire family of wavelets $\{\psi_{u,v}(x), u \in \mathbb{R}^+, v \in \mathbb{R}\}$ can be generated via the transformation

$$\psi_{u,v}(x) = u^{-1/2} \psi\{u^{-1}(x - v)\} = \psi(u, x - v) \quad (15)$$

preserving the properties in (14), for all $u \in \mathbb{R}^+$ and $v \in \mathbb{R}$. In (15) we also introduce the notation $\psi(\cdot, \cdot)$, making the dependence on scale more explicit, with $\psi(x) = \psi(1, x)$. For more information on the continuous wavelet transform, see [35].

In continuous time, we assume knowledge of the entire path rather than a finite set of observations. Consequently, it becomes irrelevant to define a sequence of stochastic processes corresponding to increasing amounts of data becoming available. Hence, continuous-time locally stationary wavelet process are defined as follows.

Definition 1. A Continuous Time Locally Stationary Wavelet Process, $\{X(t)\}_{t \in \mathbb{R}}$ is a stochastic process defined in the mean square sense as

$$X(t) = \int_0^\infty \int_{-\infty}^\infty W(u, v) \psi(u, v - t) L(du, dv), \quad (16)$$

where L is a homogeneous square-integrable Lévy basis with $\mathbb{E}[L(A)] = 0$ and $\mathbb{E}[L(A)^2] = \text{Leb}(A)$ for all $A \in \mathcal{B}_b(\mathbb{R}^+ \times \mathbb{R})$, $\{\psi_{u,v}(x), u \in \mathbb{R}^+, v \in \mathbb{R}\}$ is a continuous wavelet family as defined above and $W \in L^2(\mathbb{R}^+, \mathbb{R})$ is an amplitude function. Further, the following conditions on W hold:

- (a) For each fixed scale $u \in \mathbb{R}^+$, $W(u, \cdot)$ is a Lipschitz continuous function with Lipschitz constant $K(u)$. The Lipschitz constant function $K(u)$ is bounded and satisfies

$$\int_0^\infty uK(u)du < \infty; \quad (17)$$

- (b) For each fixed $v \in \mathbb{R}$, $W(\cdot, v)$ satisfies

$$\int_0^\infty |W(u, v)|^2 du < \infty. \quad (18)$$

Model Interpretation: Locally stationary time series are stochastic processes whose statistical properties vary slowly with time. The use of wavelets allows us to implicitly obtain a local representation and the smoothness assumptions imposed on W ensure that locally the process behaves in an approximately stationary fashion. (17) guarantees that the rate at which the statistical properties are allowed to vary decreases as the scales become wider. This insures that the process behaves in a realistic fashion and is required when one wants perform estimation.

For representation (16) to converge in mean square, the amplitude functions cannot be allowed to grow arbitrarily with u . Hence, assumption (b) ensures that $|W(u, v)|^2 \rightarrow 0$ as $u \rightarrow \infty$.

The requirement that the Lévy basis is homogeneous is essential, as this implies that the basis is stationary (and vice-versa, see Supplementary Materials Section A or [26]). This ensures that the non-stationarity is controlled entirely by the amplitude functions W . Furthermore, since L is by definition independent when acting on disjoint sets, any correlation structure in the process is captured only by the wavelets themselves.

Remark 1. The amplitude function $W(u, v)$ is defined for all $v \in \mathbb{R}$ as opposed to its discrete counterpart, which is only defined on $(0, 1)$. Later, in Section 4, when adapting this definition for practical applications, we will again return to the concept of rescaled time.

We now give an example of a continuous time locally stationary Haar wavelet process.

Definition 2. Let $u \in \mathbb{R}^+$, $x \in \mathbb{R}$ be the scale and location respectively. The **Haar Wavelet** is defined by

$$\psi_H(u, x) = u^{-1/2} \left\{ \mathbb{1}_{[0, \frac{u}{2}]}(x) - \mathbb{1}_{[\frac{u}{2}, u]}(x) \right\}. \quad (19)$$

where $\mathbb{1}$ is the usual indicator function.

Haar wavelets provide the basic building blocks for constructing the Haar moving average processes:

Example 1. A Haar Moving Average MA(α) Process is a continuous time locally stationary wavelet process $X(t)$ with amplitude function $W(u, v) = 1$ for $u = \alpha \in \mathbb{R}^+$ and zero otherwise. The Lévy basis is given by $L(du, dv) = \delta_\alpha(du)G(dv)$, where δ_α is the Dirac measure centred at α and G is a homogeneous Gaussian Lévy basis on $\mathcal{B}_b(\mathbb{R})$. The underlying wavelet family $\{\psi_{u,v}\}$ is derived from the Haar wavelet through $\psi(x) = \psi_H(-x)$, with the reflection about the y-axis chosen to maintain a backward-looking process. The Haar Moving Average MA(α) Process can be written as

$$X(t) = \int_0^\infty \int_{-\infty}^\infty \psi_H(u, v - t) \delta_\alpha(du) G(dv) = \alpha^{-1/2} [(B_t - B_{t-\alpha/2}) - (B_{t-\alpha/2} - B_{t-\alpha})], \quad (20)$$

where B_t is a standard Brownian motion. Essentially, Haar moving average processes capture the difference between consecutive Brownian increments, each of width $\alpha/2$. See [9] for the discrete time analogue, e.g. the Haar MA(1) and MA(2) processes are

$$X_t^1 = 2^{-1/2}(\varepsilon_t - \varepsilon_{t-1}) \quad \text{and} \quad X_t^2 = 2^{-1}(\varepsilon_t + \varepsilon_{t-1} - \varepsilon_{t-2} - \varepsilon_{t-3}), \quad (21)$$

respectively, where $\{\varepsilon_t\}_{t \in \mathbb{Z}}$ is an i.i.d. random variable sequence with zero mean and unit variance.

3.1 Continuous Time Evolutionary Wavelet Spectrum

The evolutionary wavelet spectrum gives a location-scale decomposition of the spectral power of a continuous time locally stationary wavelet process, and is defined as follows.

Definition 3. The **Continuous Time Evolutionary Wavelet Spectrum**, S , of a locally stationary wavelet process $X(t)$, with respect to the wavelet family ψ , is defined by

$$S(u, v) = |W(u, v)|^2, \quad (22)$$

for all scales $u \in \mathbb{R}^+$ and times $v \in \mathbb{R}$.

Assumption (b) in Definition 1 implies that, for each fixed $v \in \mathbb{R}$,

$$\int_0^\infty S(u, v) du < \infty. \quad (23)$$

Remark 2. More generally and technically, we can define

$$S^{(I)}(du, dv) = \mathbb{E} [|W(u, v)L(du, dv)|^2], \quad (24)$$

where $S^{(I)}$ is the continuous time integrated evolutionary wavelet spectrum, which we can also write as

$$S^{(I)}(du, dv) = S(u, v) du dv, \quad (25)$$

since L is a homogeneous Lévy basis. Hence,

$$S^{(I)}(u, v) = \int_0^u \int_{-\infty}^v S^{(I)}(dx, dy) = \int_0^u \int_{-\infty}^v S(x, y) dx dy, \quad (26)$$

which is not necessarily finite and is therefore of little use. One could instead define

$$S_v^{(I)}(u) = \int_0^u S(x, v) dx = \frac{\partial S^{(I)}}{\partial v}(u, v), \quad (27)$$

representing the contribution to the total power of the process in a neighbourhood of v for scales less than or equal to u . This localised integrated evolutionary wavelet spectrum mirrors the evolutionary power spectrum of [7].

Example 1 – continued. The evolutionary wavelet spectrum of a Haar MA(α) process is given by

$$S(u, v) = \begin{cases} 1, & \text{for } u = \alpha, \\ 0, & \text{for } u \neq \alpha, \end{cases} \quad (28)$$

for all $v \in \mathbb{R}$.

3.2 Continuous Time Local Autocovariance

[9] show that the autocovariance of a locally stationary wavelet process has a wavelet representation, known as the local autocovariance. We investigate continuous time versions and begin with continuous time autocorrelation wavelets, see [36].

Definition 4. For $u \in \mathbb{R}^+$ and $\tau \in \mathbb{R}$, the **Continuous Time Autocorrelation Wavelets** are defined by

$$\Psi(u, \tau) = \int_{-\infty}^{\infty} \psi(u, v)\psi(u, v - \tau)dv. \quad (29)$$

Definition 5. For time $t \in \mathbb{R}$ and lag $\tau \in \mathbb{R}$, the **Continuous Time Local Autocovariance** is defined by

$$c(t, \tau) = \int_0^{\infty} S(u, t)\Psi(u, \tau)du, \quad (30)$$

where $S(u, t)$ and $\Psi(u, \tau)$, $u \in \mathbb{R}^+$, are the continuous time evolutionary wavelet spectrum and autocorrelation wavelets, respectively.

The usual autocovariance function of a continuous time locally stationary wavelet processes is given by

$$c_X(t, \tau) = \text{cov}[X(t), X(t + \tau)] = \mathbb{E}[X(t)X(t + \tau)], \quad (31)$$

since $X(t)$ has zero mean. This can also be written in terms of the evolutionary wavelet spectrum and the underlying wavelets of the process as

$$c_X(t, \tau) = \int_0^{\infty} \int_{-\infty}^{\infty} S(u, t + v)\psi(u, v)\psi(u, v - \tau) dv du. \quad (32)$$

See Supplementary Materials Section E Proposition 1 for proof. Comparing (30) and (32), we see that the local autocovariance effectively replaces $S(u, t + v)$ with the constant $S(u, t)$ (as a function of v). The wavelet terms ensure that this is only the case over a finite interval centred at t and of width equal to that of the wavelet. Given the slow evolution of the statistical properties of the process, $S(u, t + v)$ does not differ significantly from $S(u, t)$ within this region. Although the width of this interval increases linearly in u , the speed at which S can evolve rapidly decreases to zero, since $K(u) \rightarrow 0$. If the process is stationary, the spectrum does not depend on time and the two expressions are equivalent. Therefore the local autocovariance assumes that the spectrum is locally constant, i.e. that the process is stationary at a local level, a concept which underpins the framework of locally stationary processes. This is similar to the discrete time local autocovariance defined in [9].

The next proposition establishes a bound on the maximum difference between the two expressions (30) and (32).

Proposition 1. Let $\{X(t)\}_{t \in \mathbb{R}}$ be a continuous time locally stationary wavelet process, $c_X(t, \tau)$ be its autocovariance function and $c(t, \tau)$ its local autocovariance. Then,

$$|c_X(t, \tau) - c(t, \tau)| \leq \gamma \int_0^{\infty} uK(u) du, \quad (33)$$

for all scales $u \in \mathbb{R}^+$ and times $v \in \mathbb{R}$, where γ is a constant which depends on the decay structure of the wavelet ψ and $K(\cdot)$ is the Lipschitz constant function from Definition 1.

In essence, the more stationary the process $X(t)$ is, the closer $c_X(t, \tau)$ and $c(t, \tau)$ will be, since $\int_0^{\infty} uK(u) du$ can be interpreted as a measure of the non-stationarity of the process. For a more local bound, if the spectrum S admits a Taylor series representation, we can write

$$S(u, t + v) = S(u, t) + v \frac{\partial S}{\partial v}(u, t) + o(v^2), \quad (34)$$

for v close to t . Using this expansion we can write

$$|c_X(t, \tau) - c(t, \tau)| \leq \gamma \int_0^{\infty} u \left| \frac{\partial S}{\partial v}(u, t) \right| du + M, \quad (35)$$

where $M \geq 0$ is a constant which bounds the discrepancy due to the higher order terms. From the above expression it becomes clearer that the difference between the $c_X(t, \tau)$ and $c(t, \tau)$ depends on the local structure of the process.

Remark 3. A comparison of the local and standard autocovariance functions on a simple example can be found in the Supplementary Materials Section C.

From the local autocovariance we can also define the local autocorrelation as follows.

Definition 6. The **Continuous Time Local Autocorrelation** is defined as

$$\rho(t, \tau) = \sigma^{-2}(t)c(t, \tau), \quad (36)$$

for all $t, \tau \in \mathbb{R}$, where $\sigma^2(t) = c(t, 0) = \int_0^\infty S(u, t) du$ is the local variance of the process $X(t)$ and $c(t, \tau)$ the local autocovariance defined above.

Example 1 - continued. For the Haar MA(α) processes, we have

$$c(t, \tau) = \Psi(\alpha, \tau) = c_X(t, \tau), \quad (37)$$

where Ψ is the Haar autocorrelation wavelet, see Supplementary Materials Section B. Since Haar MA processes are stationary, the local and standard autocovariance functions are equivalent. Further, $\rho(t, \tau) = c(t, \tau)$, since $\Psi(\alpha, 0) = 1$, as shown in Proposition 2.

Remark 4. *Strictly speaking, since the Dirac measure is not continuous with respect to the Lebesgue measure, (37) is calculated using*

$$c(t, \tau) = \int_0^\infty \Psi(u, \tau) S_t^{(I)}(du) = \int_0^\infty \Psi(u, \tau) \delta_\alpha(du) = \Psi(\alpha, \tau) \quad (38)$$

instead, where $S_t^{(I)}$ is defined in (27).

To conclude this section we list some useful properties of autocorrelation wavelets.

Proposition 2. Let $\Psi(u, \tau)$, $u \in \mathbb{R}^+$, denote the autocorrelation wavelets and let $\Psi(\tau) = \Psi(1, \tau)$. Then, for all $u \in \mathbb{R}^+$:

- (a) $\Psi(u, \tau)$ is symmetric as a function of τ , $\Psi(u, \tau) = \Psi(u, -\tau)$,
- (b) $\Psi(u, 0) = 1$,
- (c) $\Psi(u, \tau) = \Psi(\tau/u)$,
- (d) $\hat{\Psi}(u, \omega) = u|\hat{\psi}(u\omega)|^2$, where $\hat{\Psi}(u, \omega)$ is the Fourier transform of $\Psi(u, t)$,
- (e) $\int_{-\infty}^\infty \Psi(u, \tau) d\tau = 0$.

3.3 Relationship between the (Wavelet) Periodogram and Spectrum

We now define the raw wavelet periodogram and its relationship to the evolutionary wavelet spectrum. First, we need to define the wavelet coefficients and raw wavelet periodogram of the process.

Definition 7. The **Wavelet Coefficients** of the process $X(t)$ in terms of the wavelet basis ψ are defined as

$$d(u, v) = \int_{-\infty}^\infty X(t)\psi(u, t-v)dt, \quad (39)$$

for all scales $u \in \mathbb{R}^+$ and times $v \in \mathbb{R}$.

Definition 8. The **Raw Wavelet Periodogram** of the process $X(t)$ is defined as

$$I(u, v) = |d(u, v)|^2, \quad (40)$$

for all $u \in \mathbb{R}^+$ and $v \in \mathbb{R}$ and where $d(u, v)$ are the wavelet coefficients. Define the notation $\beta(u, v) = \mathbb{E}[I(u, v)]$, which turns out to be useful.

Before going further, we introduce the continuous counterpart of the inner product matrix defined in [9], the inner product kernel.

Definition 9. For $u, x \in \mathbb{R}^+$, the **Inner Product Kernel** is defined as

$$A(u, x) = \int_{-\infty}^\infty \Psi(u, y)\Psi(x, y) dy. \quad (41)$$

Proposition 3. The inner product kernel A is continuous, symmetric and non-negative definite. Furthermore, for all $b > 0$ and $x, y \in \mathbb{R}^+$,

$$A(bx, by) = bA(x, y). \quad (42)$$

The following theorem establishes a relationship between the expected value of the raw wavelet periodogram and an integral involving the evolutionary wavelet spectrum and inner product kernel, paralleling and extending the one of [9].

Theorem 1. *Let $\beta(u, v)$ be the expectation of the raw wavelet periodogram $I(u, v)$ of the locally stationary wavelet process $X(t)$, $S(u, v)$ its corresponding evolutionary wavelet spectrum and $A(u, x)$ the inner product kernel. Then*

$$\left| \beta(u, v) - \int_0^\infty A(u, x) S(x, v) dx \right| \leq \gamma \int_0^\infty x K(x) dx, \quad (43)$$

for all scales $u \in \mathbb{R}^+$ and times $v \in \mathbb{R}$, where γ is a constant which depends on the decay structure of the wavelet ψ and $K(\cdot)$ is the Lipschitz constant function from Definition 1.

As for Proposition 1, if $X(t)$ is stationary, then the two terms on the left hand side of (43) are equivalent. The expectation of the raw wavelet periodogram can be written as

$$\beta(u, v) = \int_0^\infty \int_{-\infty}^\infty S(x, y+v) \left(\int_{-\infty}^\infty \psi(x, y-t) \psi(u, t) dt \right)^2 dy dx, \quad (44)$$

as derived in Supplementary Materials Section D in the proof of Theorem 1. Hence $\int_0^\infty S(x, v) A(u, x) dx$ can be viewed as approximating the expectation of the raw wavelet periodogram under the assumption that $S(u, t+v) = S(u, t)$ at a local level, in the same way that the local autocovariance approximates the autocovariance. Because a similar discussion follows Proposition 1, we omit a more detailed analysis here for brevity.

Remark 5. *Equation (44), contains expressions resembling those of the cross-scale autocorrelation wavelets in the discrete setting, see [37].*

3.4 Solving for the Spectrum and Related Quantities

Theorem 1 motivates the following definition:

Definition 10. The **Inner Product Operator** is a linear integral operator $T_A : L^2(\mathbb{R}^+) \mapsto L^2(\mathbb{R}^+)$ defined by

$$(T_A f)(x) = \int_0^\infty A(x, y) f(y) dy, \quad (45)$$

for $f \in L^2(\mathbb{R}^+)$ and where $A(x, y)$ is the inner product kernel.

Theorem 1 and Definition 10 suggest that one could approximate $\beta(u, v)$ by

$$\beta(u, v) \approx \int_0^\infty A(u, x) S(x, v) dx = \{T_A S(\cdot, v)\}(u). \quad (46)$$

Therefore, given $\beta(u, v)$ we could invert the above linear integral equation to obtain the evolutionary wavelet spectrum as solution \tilde{S} . We now show how this could be done using the properties of the inner product kernel and Mercer's theorem [31]: this is a key difference with the earlier discrete time version in [9].

Since T_A has a continuous symmetric kernel, it is compact, bounded and self-adjoint. Further, we can show:

Proposition 4. *Let T_A be the linear integral operator from Definition 10. Then T_A has trivial null space, i.e. $N(T_A) = \{f \in L^2(\mathbb{R}^+) : T_A f = 0\} = \{0\}$.*

Following the discussion in Section 2, since the inner product kernel is continuous, symmetric and non-negative definite we can apply Mercer's theorem [31] to obtain a decomposition of A of the form

$$A(x, y) = \sum_{n=1}^\infty \lambda_n \varphi_n(x) \varphi_n(y), \quad (47)$$

where λ_n and φ_n are the eigenvalues and eigenfunctions of T_A . Therefore

$$(T_A f)(x) = \sum_{n=1}^\infty \lambda_n \langle \varphi_n, f \rangle \varphi_n(x), \quad (48)$$

where

$$\langle f, g \rangle = \int_0^\infty f(x) g(x) dx \quad (49)$$

for $f, g \in L^2(\mathbb{R}^+)$. Since T_A is self-adjoint, this allows us to obtain the solution

$$\tilde{S}(u, t) = \sum_{n=1}^{\infty} \lambda_n^{-1} \langle \beta(\cdot, t), \varphi_n(\cdot) \rangle \varphi_n(u), \quad (50)$$

to the linear integral equation (46), for all $u \in \mathbb{R}^+$ and $t \in \mathbb{R}$, which is unique, due to the fact that $N(T_A) = \{0\}$.

The evolutionary wavelet spectral solution (50) can be used to obtain an estimate of the local autocovariance using (30). Furthermore, the ability to invert T_A also permits us to invert (30) to obtain a representation of the spectrum in terms of the local autocovariance as follows:

Theorem 2. *Let $c(t, \tau)$ be the local autocovariance of a continuous time locally stationary wavelet process. Then the evolutionary wavelet spectrum can be written as*

$$S(u, t) = \int_{-\infty}^{\infty} B(u, \tau) c(t, \tau) d\tau, \quad (51)$$

where

$$B(u, \tau) = \sum_{n=1}^{\infty} \lambda_n^{-1} \langle \Psi(\cdot, \tau), \varphi_n(\cdot) \rangle \varphi_n(u), \quad (52)$$

Ψ is an autocovariance wavelet and λ_n and φ_n are the eigenvalues and eigenvectors of the inner product operator T_A from Definition 10.

We note that, so far, we have ignored the fact that generally one does not work directly with $\beta(u, v)$, but rather with a realisation, or in some cases a set of samples, of the locally stationary wavelet process $X(t)$, which can then be used to obtain an estimate of $\beta(u, v)$. This, of course, introduces noise into the linear integral equation. To address this problem, regularisation methods such as the spectral cut-off method discussed in Section 2 can be employed.

We now consider the practical situation where we only have access to a discrete sample of points and focus on techniques to estimate quantities from these.

4 Implementation of Spectral and Autocovariance Estimators

In practice, one typically has access to a discrete and finite realisation of the process, rather than the entire sample path. Therefore, estimation of spectral and autocovariance quantities requires adaptations of the previous section's theoretical framework. To begin, we provide a new definition of locally stationary wavelet processes in continuous time, reintroducing a sequence of stochastic processes and the concept of rescaled time.

Definition 11. Let $n(T)$ be a non-decreasing integer valued function of $T \in \mathbb{R}^+$, such that $n(T) \rightarrow \infty$ as $T \rightarrow \infty$, and $\mathcal{T} = \{t_0, t_1, \dots, t_{n(T)-1}\}$ be a set of times, such that $0 = t_0 < t_1 < \dots < t_{n(T)-1} = T$. A sequence of stochastic processes $\{X_T(t)\}_{t \in \mathcal{T}}$ indexed by T is said to be a **Sampled Continuous Time Locally Stationary Wavelet Process** if it admits the representation

$$X_T(t) = \int_0^{J_\psi(T)} \int_{-\infty}^{\infty} w_T(u, v) \psi(u, v - t) L(du, dv), \quad (53)$$

in the mean square sense, where L is a square-integrable homogeneous Lévy basis with $\mathbb{E}[L(A)] = 0$ and $\mathbb{E}[L(A)^2] = \text{Leb}(A)$ for all $A \in \mathcal{B}_i(\mathbb{R}^+ \times \mathbb{R})$, $\{\psi_{u,v}(x), u \in \mathbb{R}^+, v \in \mathbb{R}\}$ is a continuous wavelet family, $w_T \in L^2(\mathbb{R}^+, \mathbb{R})$ is a sequence of location-scale amplitude functions and $J_\psi(T)$ is an increasing function which depends on the wavelet ψ . Further, there exists a function $W : \mathbb{R}^+ \times (0, 1) \mapsto \mathbb{R}$ such that:

- (a) For each fixed scale $u \in \mathbb{R}^+$, $W(u, \cdot)$ is a Lipschitz continuous function with Lipschitz constant $K(u)$. The Lipschitz constant function $K(\cdot)$ is bounded and satisfies

$$\int_0^{\infty} u K(u) du < \infty. \quad (54)$$

- (b) For each fixed $z \in (0, 1)$, $W(\cdot, z)$ satisfies

$$\int_0^{\infty} |W(u, z)|^2 du < \infty. \quad (55)$$

(c) For each fixed scale $u \in \mathbb{R}^+$ there exists a constant $C(u)$ such that for each $T \in \mathbb{R}^+$

$$\sup_{v \in \mathcal{T}} \left| w_T(u, v) - W\left(u, \frac{v}{T}\right) \right| \leq \frac{C(u)}{T} \quad \text{and} \quad \int_0^\infty C(u) du < \infty. \quad (56)$$

Model Interpretation: We have now reintroduced the concept of rescaled time, $z = v/T \in (0, 1)$, as is standard in the literature on locally stationary processes, see [8] for example. In essence, this means that as $T \rightarrow \infty$ we are collecting increasing amounts of data and so are learning more and more about the local structure of the process. Assumption (c) formalises this notion, ensuring that $w_T(u, v)$ converges to its rescaled time limit $W(u, v/T)$, while also becoming smoother in the process. In our setting, the growing number of observations is given by $n(T)$, whereas T now denotes the total length of the data. Thus, we still rescale the process by T , with the increased flexibility of being able to handle irregularly spaced observations.

The function $J_\psi(T)$ determines the maximum scale that contributes to the process. As more data becomes available, the model is able to include increasingly coarser scales and so $J_\psi(T) \rightarrow \infty$ as $T \rightarrow \infty$. We make the dependence of $J_\psi(T)$ on the structure of the underlying wavelet explicit by including ψ in the subscript.

Continuous wavelets can be defined for any scale in \mathbb{R}^+ and can be shifted to any location in \mathbb{R} . This makes the continuous wavelet transform particularly well suited for handling missing observations or irregularly spaced data.

We now redefine the evolutionary wavelet spectrum in this setting:

Definition 12. The **Evolutionary Wavelet Spectrum** of the sampled continuous time locally stationary wavelet process, $X_T(t)$, with respect to ψ is defined by

$$S(u, z) = |W(u, z)|^2, \quad (57)$$

for all $u \in \mathbb{R}^+$ and $z = v/T \in (0, 1)$.

Definition 11 (b) and (c), imply that, for each fixed $z \in (0, 1)$,

$$\int_0^\infty S(u, z) du < \infty \quad \text{and} \quad S(u, z) = \lim_{T \rightarrow \infty} |w_T(u, v)|^2, \quad (58)$$

for all $u \in \mathbb{R}^+$ and $v \in \mathbb{R}$.

The local autocovariance and autocorrelation remain as before, except that we replace t with its rescaled version z , as was done for the evolutionary wavelet spectrum above. To emphasize the dependence on T , we now denote the autocovariance by $c_{X_T}(t, \tau)$.

Proposition 1 highlighted the discrepancy between the ‘regular’ autocovariance $c_X(t, \tau)$ from (31) and the ‘wavelet’ autocovariance $c(t, \tau)$ from (30) for the theoretical process with equality in the stationary case. However, in the sampled case, the autocovariances become close asymptotically, as shown by the following.

Proposition 5. Let $\{X_T(t)\}_{t \in \mathcal{T}}$ be a sampled continuous time locally stationary wavelet process, $c_{X_T}(t, \tau)$ its autocovariance function, $c(z, \tau)$ the local autocovariance and $z = t/T$. Then we obtain the following bound

$$|c_{X_T}(t, \tau) - c(z, \tau)| = O(T^{-1}) \quad (59)$$

In other words, the autocovariance converges to the local autocovariance as $T \rightarrow \infty$.

4.1 Estimation Theory

The wavelet coefficients are defined as in (39), while the raw wavelet periodogram is now defined in rescaled time $z = v/T$ as

$$I(u, z) = I\left(u, \frac{v}{T}\right) = |d(u, v)|^2 = |d(u, zT)|^2. \quad (60)$$

As in Definition 8, we again use the notation $\beta(u, z) = \mathbb{E}[I(u, z)]$.

This leads us to the following result:

Theorem 3. Let $I(u, z)$ be the raw wavelet periodogram of the sampled continuous time locally stationary wavelet process $X_T(t)$, $S(u, z)$ its corresponding evolutionary wavelet spectrum and $A(u, x)$ the inner product kernel. Then

$$\left| \beta(u, z) - \int_0^{J_\psi(T)} A(u, x) S(x, z) dx \right| = O(T^{-1}) \quad (61)$$

and

$$\left| \text{Var} [I(u, z)] - 2 \left[\int_0^{J_\psi(T)} A(u, x) S(x, z) dx \right]^2 \right| = O(uT^{-1}) \quad (62)$$

for all $u \in (0, J_\psi(T)]$ and $z \in (0, 1)$.

Equation (61) suggests estimating spectrum, S , by solving the linear integral equation

$$\beta(u, z) = \int_0^{J_\psi(T)} A(u, x) S(x, z) dx = \{T_A S(\cdot, z)\}(u), \quad (63)$$

using estimates of β , denoted $\hat{\beta}$, on which we elaborate in Section 4.2, where

$$(T_A f)(x) = \int_0^{J_\psi(T)} A(x, y) f(y) dy. \quad (64)$$

Note that the same properties hold for this linear integral operator as for its theoretical counterpart defined in (45). The use of an estimate of β naturally introduces noise into (63). Hence, to compute an estimate \hat{S} of the spectrum S , we use the iterative algorithm developed in [33] and described in Section 2. This involves reformulating (63) as a minimisation problem with the aim of minimising the discrepancy

$$\Delta S(\cdot, z) = \left\| T_A S(\cdot, z) - \hat{\beta}(\cdot, z) \right\|_2^2 + \mu \|S(\cdot, z)\|_1, \quad (65)$$

for each $z \in (0, 1)$, where $\|\cdot\|_1$ and $\|\cdot\|_2$ denote the $L^1(\mathbb{R}^+)$ and $L^2(\mathbb{R}^+)$ norms respectively and $\mu > 0$ is the regularisation parameter. By definition the evolutionary wavelet spectrum is a non-negative quantity and so we use asymmetric soft thresholding. Hence, in this setting, we reformulate the iterative scheme as

$$\hat{S}^n(\cdot, z) = \text{Shrink}_{\mu,1} \left\{ \hat{S}^{n-1}(\cdot, z) + T_A [\hat{\beta}(\cdot, z) - T_A \hat{S}^n(\cdot, z)] \right\}, \quad n = 0, \dots, N, \quad (66)$$

where N is the number of iterations and

$$(\text{Shrink}_{\mu,1} f)(x) = \begin{cases} f(x) - \mu/2, & \text{if } f(x) \geq \mu/2, \\ 0, & \text{if } f(x) < \mu/2, \end{cases} \quad (67)$$

which, as shown in [33], converges strongly to the unique minimiser of (65).

Remark 6. We have implicitly chosen to penalise the function values directly when imposing the constraint in (65) and, subsequently, when defining the $\text{Shrink}_{\mu,1}$ operator. This makes guaranteeing the non-negativity of the spectrum straightforward and is equivalent to selecting the standard basis in (11).

Note that we have replaced T_A^\dagger with T_A in (66), as T_A^\dagger is by definition self-adjoint.

4.2 Practical Considerations

Here, we begin by explaining why we choose the [33] iterative thresholding algorithm through a simple comparison with Tikhonov regularisation. When we can access the actual (theoretical) value of β , Tikhonov regularisation is the natural choice for inverting (63), both in terms of accuracy and computational efficiency (see top row of Figure 1). However, access to the true β is rarely available and as soon as we work with estimates, its performance rapidly deteriorates, no longer guaranteeing the non-negativity of the evolutionary wavelet spectrum. Therefore, in general, the [33] iterative thresholding algorithm described earlier is our preferred choice, as it remains robust against noise contamination (see second figure from the left in the bottom row of Figure 1).

When discretising the various quantities of interest, we assume that we are given observations of a process at times $0 = t_0 < t_1 < \dots < t_{n(T)-1} = T$, with $n(T)$ from Definition 11. The continuous wavelet transform can be computed for arbitrary scales u and shifts v , without being restricted by the structure of the time series data. Hence, we opt to do so using a regularly spaced grid. We select scales $u_0 < u_1 < \dots < u_{M_u-1} = J_\psi(T)$ and locations $0 = v_0 < v_1 < \dots < v_{M_v-1} = T$, such that $u_i - u_{i-1} = \Delta u$ and $v_j - v_{j-1} = \Delta v$ for $i = 1, \dots, M_u - 1$, $j = 1, \dots, M_v - 1$ and $M_u, M_v \in \mathbb{N}$. In general, we choose an M_v which matches the number of available observations, growing linearly with T . The wavelet coefficients (39) can then be approximated as

$$d(u_i, v_j) \approx \frac{1}{2} \sum_{k=1}^{n(T)-1} \{X_T(t_k) \psi(u_i, t_k - v_j) + X_T(t_{k-1}) \psi(u_i, t_{k-1} - v_j)\} \Delta t_k, \quad (68)$$

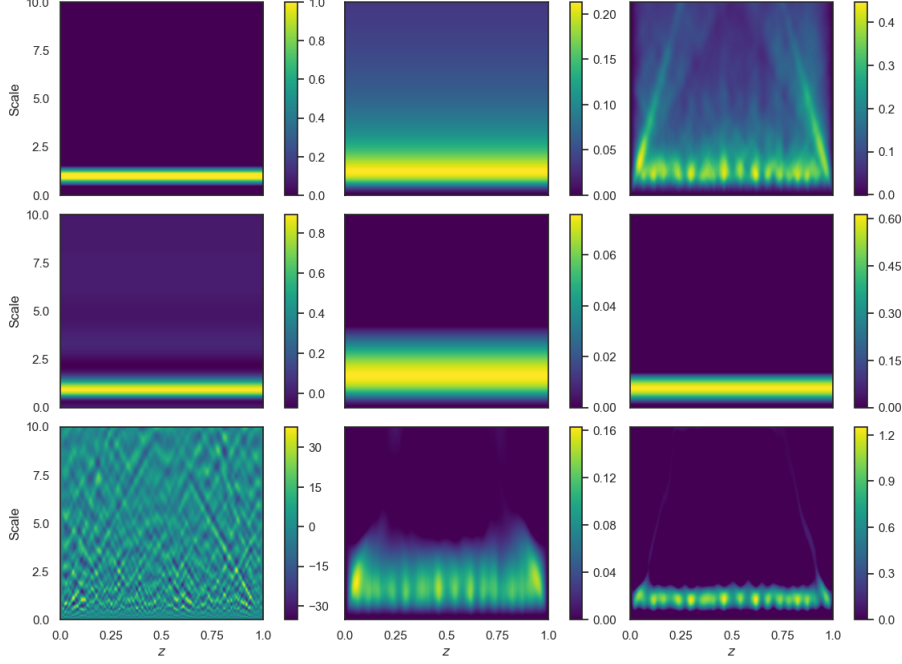


Figure 1: A comparison of Tikhonov regularisation and [33]’s iterative thresholding algorithm when β is known (middle row) and when it is estimated from the data (bottom row). Top left: the true evolutionary wavelet spectrum. Top centre: the true raw wavelet periodogram. Top right: an estimate of the raw wavelet periodogram. Middle and bottom rows, from left to right: solution using Tikhonov regularisation, solutions from running the [33] iterative thresholding algorithm for 100 and 10000 iterations.

or equivalently as

$$d(u_i, v_j) \approx \frac{1}{2} \sum_{k=0}^{n(T)-1} X_T(t_k) \psi(u_i, t_k - v_j) \tilde{\Delta} t_k, \quad (69)$$

where $\Delta t_k = t_k - t_{k-1}$ and $\tilde{\Delta} t_k = t_{k+1} - t_{k-1}$. The corresponding discretised raw wavelet periodogram is then given by

$$I(u_i, z_j) = |d(u_i, v_j)|^2, \quad (70)$$

where $z_j = v_j/T$.

Remark 7. *It is not strictly necessary to restrict the discretisation procedure to a regularly spaced grid. However, doing so for the locations v proves particularly useful when applying smoothing techniques, as described in Section 4.3.*

Using the same grid, the inner product operator in (64) can be approximated as

$$\{T_A S(\cdot, z_j)\}(u_i) \approx \Delta u \sum_{k=0}^{M_u-1} A(u_i, u_k) S(u_k, z_j) \quad (71)$$

and then used to obtain an estimate of the evolutionary wavelet spectrum $\hat{S}(u_i, z_j)$ from $\hat{\beta}(u_i, v_j)$ using the iterative scheme in (66). From $\hat{S}(u_i, z_j)$ we can also compute an estimate of the local autocovariance using

$$\hat{c}(z_j, \tau) \approx \Delta u \sum_{i=0}^{M_u-1} \hat{S}(u_i, z_j) \Psi(u_i, \tau), \quad (72)$$

for appropriately chosen lags τ , as well as the local autocorrelation.

Throughout this work, we have mentioned that, in practice, we generally work with an estimate $\hat{\beta}$ of β . In most situations, we only have a single realisation of the process, $X_T(t)$, and thus our best estimate would simply be our

discretised raw wavelet periodogram from equation (70), i.e. $\hat{\beta}(u, z) = I(u, z)$. However, there are situations where we may have access several realisations of the same process, known as replicated time series, see [38] and [39] for example, and can set

$$\hat{\beta}(u, z) = R^{-1} \sum_{i=1}^R I_i(u, z), \quad (73)$$

where R is the number of replicates and $I_i(u, z)$ denotes the raw wavelet periodogram for the i -th realisation. Here we again see the strength of the continuous wavelet transform, in that (73) can be computed regardless of whether the grid structure of the individual time series match.

When initialising the [33] iterative algorithm in (10), we set $S^0(u, z) = \hat{\beta}(u, z)$. As described in [33] and Section 2, denoting the noise level by ε , one should select $\mu = \mu(\varepsilon)$ such that

$$\lim_{\varepsilon \rightarrow 0} \mu(\varepsilon) = 0 \quad \text{and} \quad \lim_{\varepsilon \rightarrow 0} \varepsilon^2 / \mu(\varepsilon) = 0. \quad (74)$$

Using Theorem 3, we set

$$\mu(u, z) = \left[\text{Var} \left\{ \hat{\beta}(u, z) \right\} \right]^{\frac{1}{2}}, \quad (75)$$

which clearly satisfies the conditions in (74). This can either be set as a global parameter or can be allowed to vary as a function of u and z .

In using the [33] algorithm, we empirically observe that convergence of the spectrum at finer scales typically requires more time. This is because, given the same level of information, the size of the wavelet coefficients tends to increase as the scales become wider. Furthermore, information at wider scales also seems to exhibit greater variability, consistent with the results from Theorem 3. To address this effect, we propose to apply level-dependent universal wavelet smoothing to the raw wavelet periodogram, as we describe next.

4.3 Smoothing the Discretised Raw Wavelet Periodogram Across Time

As for the discrete setting [9], the raw wavelet periodogram is not a consistent estimator of β . A key advantage of the continuous wavelet transform is that we can compute the wavelet coefficients $d(u, v)$ on a regularly spaced grid, regardless of the time series original structure. In the following, we use the same grid as the one constructed in Section 4.2, with the exception of requiring that $M_v = 2^\eta$ for some $\eta \in \mathbb{N}$, where M_v is the number of locations. Note that M_v grows in a linear fashion with T , and so $M_v \rightarrow \infty$ as $T \rightarrow \infty$. Standard wavelet smoothing techniques using the discrete wavelet transform, see for example [18, 40, 41, 42, 43, 44] can then be applied to $\hat{\beta}$ across location in a straightforward manner, as in [9]. In the following we drop the subscript i from (70) and write u instead of u_i for simplicity.

To apply wavelet shrinkage to the discretised periodogram, we introduce an additional orthonormal discrete wavelet basis of $L^2(0, 1)$, which is different from the continuous wavelets introduced in (15) and used throughout our article above.

Definition 13. Wavelet Shrinkage Basis and Coefficients. Let $\{\tilde{\phi}_{\ell_0, m}, \tilde{\psi}_{\ell, m}\}$ be an orthonormal discrete wavelet basis of $L^2(0, 1)$ and define the mother and father wavelet coefficients of the discretised raw wavelet periodogram as

$$\tilde{d}_{\ell, m}^u = \frac{1}{M_v} \sum_{j=0}^{M_v-1} \hat{\beta}(u, z_j) \tilde{\psi}_{\ell, m}(z_j), \quad \ell = \ell_0, \dots, \eta, \quad m = 0, \dots, 2^\ell - 1, \quad (76)$$

and

$$\tilde{c}_{\ell_0, m}^u = \frac{1}{M_v} \sum_{j=0}^{M_v-1} \hat{\beta}(u, z_j) \tilde{\phi}_{\ell_0, m}(z_j), \quad m = 0, \dots, 2^{\ell_0} - 1, \quad (77)$$

where $\tilde{\psi}_{\ell, m} = 2^{\ell/2} \tilde{\psi}(2^\ell z - m)$, ψ is a wavelet function satisfying (14), $\ell = \ell_0, \dots, \eta$, $m = 0, \dots, 2^\ell - 1$ and ℓ_0 is the coarsest scale included in the scheme. The superscript u is used to indicate that each level u is smoothed separately as a function of z .

Equations (76) and (77) parallel equation (39) of [45]. As stated in [40], the finer scale coefficients are the ones which are most susceptible to noise. Hence in general, following [18], we set $\ell_0 = 3$. We can then apply a soft threshold to the wavelet coefficients $\tilde{d}_{\ell, m}^u$ to obtain estimates $\tilde{d}_{\ell, m}^{u, S}$. The resulting non-linear estimate of the raw wavelet periodogram is

then given by

$$\tilde{\beta}(u, z_j) = \sum_{m=0}^{2^{\ell_0}-1} \tilde{c}_{\ell_0, m}^u \tilde{\phi}_{\ell_0, m}(z_j) + \sum_{\ell=\ell_0}^{\eta} \sum_{m=0}^{2^{\ell}-1} \tilde{d}_{\ell, m}^{u, S} \tilde{\psi}_{\ell, m}(z_j). \quad (78)$$

The smoothed raw wavelet periodogram $\tilde{\beta}$ is then used to compute an estimate of the evolutionary wavelet spectrum \hat{S} using the [33] iterative thresholding algorithm.

The following theorem parallels that of [9].

Theorem 4. *For locally stationary wavelet processes with Gaussian Lévy basis, the wavelet coefficients $\tilde{d}_{\ell, m}^u$ are asymptotically normally distributed with*

$$\left| \mathbb{E} \left(\tilde{d}_{\ell, m}^u \right) - \int_0^1 \int_0^\infty A(u, x) S(x, z) dx \tilde{\psi}_{\ell, m}(z) dz \right| = O \left(2^{\ell/2} T^{-1} \right) \quad (79)$$

and

$$\left| \text{Var} \left(\tilde{d}_{\ell, m}^u \right) - 2T^{-1} \int_0^1 \left[\int_0^\infty A(u, x) S(x, z) dx \right]^2 \tilde{\psi}_{\ell, m}^2(z) dz \right| = O \left(2^\ell u T^{-2} \right). \quad (80)$$

Hence, following [9, 42, 43], we obtain the following result.

Theorem 5. *Define the threshold*

$$\lambda(\ell, m, u, T) = \tilde{\sigma}_{\ell, m}^u \log(T), \quad \text{with } (\tilde{\sigma}_{\ell, m}^u)^2 = \text{Var} \left(\tilde{d}_{\ell, m}^u \right). \quad (81)$$

Then, under the assumptions of Theorem 4, for each $u \in \mathbb{R}^+$,

$$\mathbb{E} \left[\int_0^1 \left| \tilde{\beta}(u, z) - \beta(u, z) \right|^2 \right] = O \left(T^{-\frac{2}{3}} \log^2(T) \right) \quad (82)$$

The above relies on the assumption that the underlying Lévy basis is Gaussian. If settings where this is not the case, one could apply the techniques described in [41]. Instead of smoothing the raw wavelet periodogram directly, one could smooth the log of the wavelet periodogram instead, a transform which is often used to stabilise the variance of a process, as noted in [9] and Remark 4.11 of [42]. Alternatively, the methods using the Haar-Fisz transform as described in [46, 47] for the discrete setting could be extended to work in the continuous case as well.

4.4 Non-Stationary Haar Moving Average Example

We now apply our methods to a set of non-stationary Haar moving average realisations. The true underlying evolutionary wavelet spectrum is displayed the upper left part of Figure 2 (for the full functional specification see Supplementary Materials Section D). We also display a sample drawn from this spectrum, as well as the true wavelet periodogram and local autocovariance, which in this case is equal to the local autocorrelation.

We draw 1000 realisations, $X_T(t)$, of a process with the Haar MA evolutionary wavelet spectrum and compute an estimate of β using (73) for $R = 1, 10, 100$ and 1000. In each case, we then use the [33] iterative algorithm to compute an evolutionary wavelet spectral estimate. The smoothing is carried out using Daubechies wavelets [35] with $N = 2$ vanishing moments. The threshold λ given by equation (81) is estimated using and applied to the coefficients ranging from level 3 to the finest scale, as outlined in [18]. The results of running this algorithm for 100, 1000 and 10000 iterations are displayed in Figure 3. As expected, results improve as we increase both the number of samples used to compute (73) and the number of iterations in the [33] iterative thresholding algorithm. As mentioned in the practical considerations, we observe that finer scale information requires a larger number of iterations to become as visible in the estimate as information at larger scales. Additionally, we notice that spectral information tends to deviate more from its true value at larger scales, again aligning with previous comments and with the results in Theorem 3.

We now use our evolutionary wavelet spectrum estimates to obtain an estimate of the local autocovariance using (72), and thence an estimate of the local autocorrelation, shown in Figure 4. For this purpose, we only use our evolutionary wavelet spectral estimate which was obtained by running the [33] iterative algorithm for 10000 iterations.

Once again, the results improve as the number of samples used to estimate β increases. Even when only one sample is employed, it is still possible to distinguish between different frequency regions, although this distinction is more apparent in the local autocorrelation estimate than in the local autocovariance. When a smaller number of samples are used, all estimates, including those of the evolutionary wavelet spectrum, display a higher degree of variability. Therefore, it may be beneficial to further investigate more appropriate smoothing techniques, an avenue which we leave for future research.

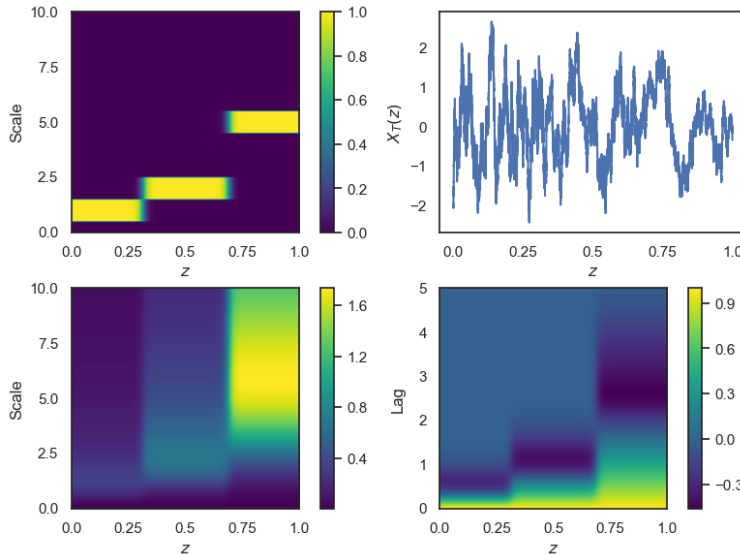


Figure 2: From left to right, top to bottom: the true evolutionary wavelet spectrum, a sample realisation, the true raw wavelet periodogram and the true local autocovariance function (which in this case is equivalent to the local autocorrelation) for the non-stationary Haar moving average process.

5 Application to Heart Rate and Sleep Stage Data

We now apply our methods to study the heart rate of a sleeping individual. The data in our study here are irregularly spaced and so the discrete time methods from [9] simply cannot be used. Existing methods [11] for dealing with irregularly-spaced data in this setting are computationally demanding and produce estimates of a very different nature to the underlying spectral quantity we want to estimate. Our new methods are the only ones to our knowledge that can produce a genuine estimate in reasonable time for irregularly-spaced data.

[48] collected data for a study to attempt to predict different sleep stages based on heart rate recordings obtained from wearable devices during sleep. The data are available at [49]. The heart rate and sleep stages of several individuals were recorded and we selected one for our analyses. The sleep stages are labelled 0 to 5, representing progressively deeper stages of sleep. Specifically, stage 0 corresponds to wakefulness, stages 1 to 3 correspond to non-rapid eye movement (NREM) sleep stages 1 to 3, and stage 5 corresponds to REM sleep. Figure 5 shows the heart rate and sleep stage of the chosen individual, which clearly exhibits non-stationary behaviour.

We fit models using Haar wavelets as the underlying wavelet functions, with scales ranging from 1 to 10000 and symmetric boundary conditions. Since the data consists of unequally spaced observations, we compute the continuous wavelet transform on an evenly spaced grid, with a spacing equal to 1 second. To compute an evolutionary wavelet spectral estimate, we employed the [33] iterative algorithm, from which we then obtained an estimate of the local autocorrelation function. Prior to estimating the evolutionary wavelet spectrum, smoothing techniques were also applied to the raw wavelet periodogram, using the same parameters as those outlined in Section 4.4.

Figure 6 displays the estimates. The evolutionary wavelet spectral estimate, is concentrated primarily at coarser scales in regions where the heart rate corresponds to deeper sleep stages, such as the NREM stage. We can clearly see three distinct peaks, which seem to align with those in the sleep stage labels plot, although the rightmost one is less visible, possibly due to boundary effects or other noise sources. A similar relationship can be observed when viewing the local autocorrelation estimate, although this is somewhat less clear. This suggests that spectral information at larger scales corresponds to deeper sleep stages, whereas information appearing at finer scales corresponds to lighter sleep.

The above suggests that such methods can provide valuable insight into the analysis of (sampled) irregularly-spaced time series, in this case heart rate and sleep stage data.

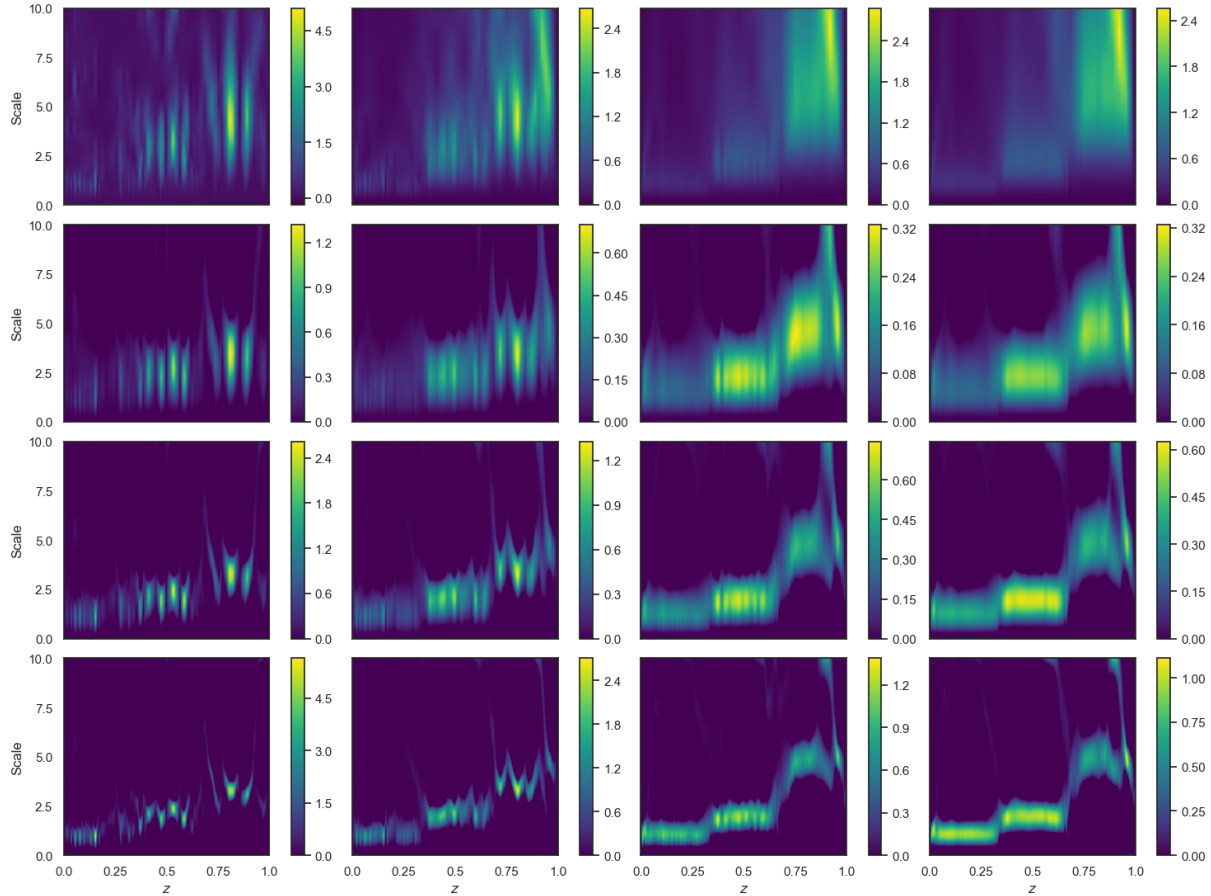


Figure 3: Estimates of the raw wavelet periodogram and corresponding evolutionary wavelet spectrum using the [33] iterative thresholding algorithm. From left to right: estimates computed using 1, 10, 100 and 1000 samples. From top to bottom: raw wavelet periodogram, evolutionary wavelet spectrum from running the iterative thresholding algorithm for 100, 1000 and 10000 iterations.

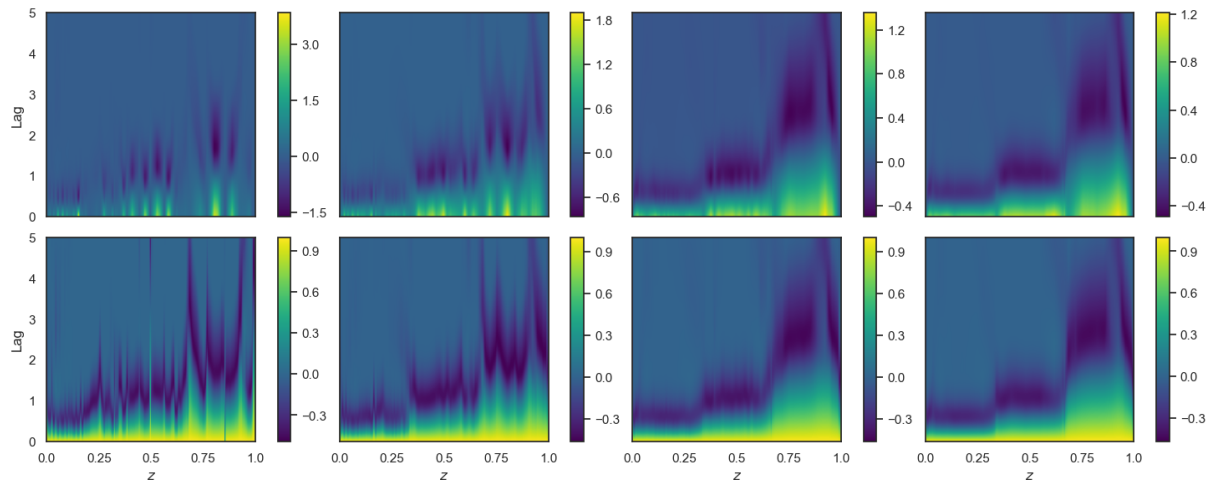


Figure 4: Local autocovariance (top row) and autocorrelation (bottom row) estimates for the non-stationary Haar moving average process using evolutionary wavelet spectral estimates obtained from running the [33] iterative algorithm for 10000 iterations. The columns are sorted in ascending order of the number of samples used to estimate $\beta(u, z)$.

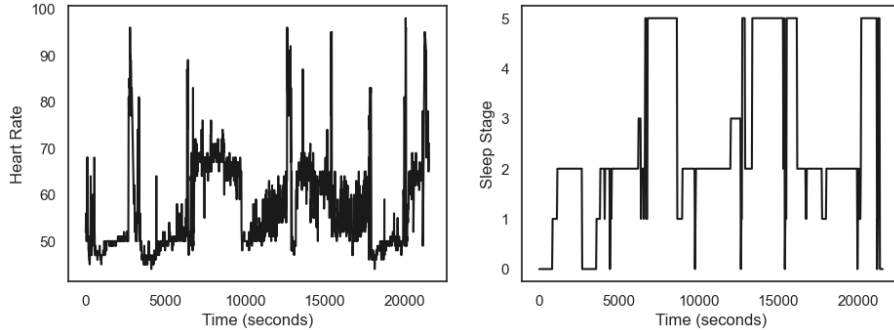


Figure 5: Heart rate of a sleeping individual (left) and corresponding sleep stage (right). Data obtained from [49]

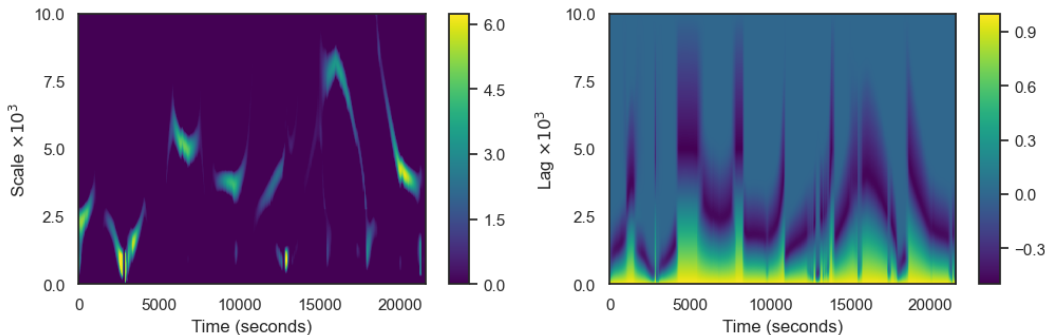


Figure 6: Estimates of the evolutionary wavelet spectrum (left) and local autocorrelation (right) for the Haar locally stationary wavelet model fitted to the heart rate data.

6 Conclusions and Future Work

This article introduces continuous time locally stationary wavelet processes along with the associated continuous time evolutionary wavelet spectra and local autocovariance. Our new methods are ideally suited for the modelling and analysis of irregularly-spaced time series data or regularly-spaced time series subject to missingness. We have introduced rigorous theory using homogeneous Lévy bases to embed our new continuous time processes and associated quantities. A key contribution is the application of the [33] iterative algorithm for solving the key linear integral equation to obtain positive spectral quantities and also deal with noise. The novel methods developed here permit accurate estimates of the evolutionary wavelet spectrum within a reasonable computational time-frame. Further, our evolutionary wavelet spectrum is inherently defined across a continuous spectrum of scales, thereby offering a more comprehensive representation of the underlying frequency information for time series, irregular or not.

Our new continuous time locally stationary wavelet process work throws up several interesting avenues for future work. First, one promising direction would be the development of improved smoothing techniques for the raw wavelet periodogram, to enable more accurate and reliable estimation of the evolutionary wavelet spectrum and local autocovariance. This is particularly relevant for processes that exhibit significant spectral power at larger scales. Second, it would be useful to investigate the impact of discrete approximations on continuous time models, particularly in relation to aliasing. The study on the effects of aliasing in the context of locally stationary wavelet processes has shown promise in detecting its absence [20, 21]. Extending these methods to the continuous time models developed in this article could yield further insights into such behaviours, which only work because of their non-stationarity. Other directions for future work could also include the development of alternative approaches or algorithms for estimating the evolutionary wavelet spectrum, and related quantities or exploring applications of these models in various fields such as finance, economics, healthcare or physics.

Acknowledgements: We would like to thank Almut Veerart for helpful discussions and feedback on an earlier version of this work.

Proofs and Code Availability: Proofs can be found in Supplementary Materials Section E. The code can be found at: <https://github.com/henrypalasciano/CLSWP>

References

- [1] P.J. Brockwell and R.A. Davis. *Time Series: Theory and Methods*. Springer, New York, 1991.
- [2] D.B. Percival and A.T. Walden. *Spectral Analysis for Univariate Time Series*. Cambridge University Press, Cambridge, 2020.
- [3] A.J. Boness, A.H. Chen, and S. Jatusipitak. Investigations of nonstationarity in prices. *J. Bus.*, 47(4):518–537, October 1974.
- [4] G. Livan, J. Inoue, and E. Scalas. On the non-stationarity of financial time series: impact on optimal portfolio selection. *J. Stat. Mech-Theory E*, 2012(07):P07025, July 2012.
- [5] T.A. Schmitt, D. Chetalova, R. Schäfer, and T. Guhr. Non-stationarity in financial time series: Generic features and tail behavior. *Europhysics Letters*, 103(5), September 2013.
- [6] P. Fryzlewicz. Modelling and forecasting financial log-returns as locally stationary wavelet processes. *J. Appl. Stat.*, 32:503–528, 07 2005.
- [7] M.B. Priestley. *Spectral Analysis and Time Series, Volumes I and II*. London: Academic Press, 1983.
- [8] R. Dahlhaus. Fitting time series models to nonstationary processes. *Ann. Statist.*, 25(1):1–37, February 1997.
- [9] G.P. Nason, R. von Sachs, and G. Kroisandt. Wavelet processes and adaptive estimation of the evolutionary wavelet spectrum. *J. R. Statist. Soc. B*, 62(2):271–292, 2000.
- [10] M.I. Knight and G.P. Nason. A ‘nondecimated’ lifting transform. *Stat. Comput.*, 19:1–16, Apr 2008.
- [11] M.I. Knight, M.A. Nunes, and G.P. Nason. Spectral estimation for locally stationary time series with missing observations. *Stat. Comput.*, 22:877–895, Jul 2011.
- [12] F.C. Drost and B.J.M. Werker. Closing the GARCH gap: Continuous time GARCH modeling. *J. Econometrics*, 74(1):31–57, 1996.
- [13] P.J. Brockwell, R.A. Davis, and Y. Yang. Continuous-time Gaussian autoregression. *Statistica Sinica*, 17(1):63–80, Jan 2007.
- [14] E. Calvello, S. Reich, and A.M. Stuart. Ensemble Kalman methods: A mean field perspective. *arXiv preprint arXiv:2209.11371*, September 2022.
- [15] L. Lucchese, M.S. Pakkanen, and A.E.D. Veraart. Estimation and inference for multivariate continuous-time autoregressive processes. *arXiv preprint arXiv:2307.13020*, July 2023.
- [16] A. Bitter, R. Stelzer, and B. Ströh. Continuous-time locally stationary time series models. *Adv. Appl. Probab.*, 55:965–998, June 2023.
- [17] R. Dahlhaus. Locally stationary processes. *Handbook of Statistics*, 30:351–413, May 2012.
- [18] G.P. Nason. *Wavelet Methods in Statistics with R*. Springer: New York, 2008.
- [19] L. Winkelmann. Forward guidance and the predictability of monetary policy: a wavelet-based jump detection approach. *J. R. Statist. Soc. C*, 65(2):299–314, 2016.
- [20] I.A. Eckley and G.P. Nason. A test for the absence of aliasing or local white noise in locally stationary wavelet time series. *Biometrika*, 105(4):833–848, 2018.
- [21] H.A. Palasciano and G.P. Nason. A test for the absence of aliasing or white noise in two-dimensional locally stationary wavelet processes. *Stat. Comput.*, 33(108), July 2023.
- [22] J. Hargreaves, M.I. Knight, J. Pitchford, R. Oakenfull, S. Chawla, J. Munns, and S. Davis. Wavelet spectral testing: Application to nonstationary circadian rhythms. *The Annals of Applied Statistics*, 13, 03 2018.
- [23] J.D. Romano and N.J. Cornish. Detection methods for stochastic gravitational-wave backgrounds: a unified treatment. *Living Rev. Relativ.*, 20(2):1–223, 2017.
- [24] J. Nowotarski, J. Tomczyk, and R. Weron. Robust estimation and forecasting of the long-term seasonal component of electricity spot prices. *Energ. Econ.*, 39:13–27, 2013.
- [25] L.M. de Menezes, M.A. Houllier, and M. Tamvakis. Time-varying convergence in European electricity spot markets and their association with carbon and fuel prices. *Energ. Policy*, 88:613–627, 2016.
- [26] O.E. Barndorff-Nielsen, F. Espen Benth, and A.E.D. Veraart. *Ambit Stochastics*. Springer, 2018.
- [27] B.S. Rajput and J. Rosinski. Spectral representations of infinitely divisible processes. *Probab. Theory Rel.*, 82:451–487, August 1989.

- [28] D. Applebaum. *Lévy Processes and Stochastic Calculus*. Cambridge Studies in Advanced Mathematics. Cambridge University Press, 2009.
- [29] J. Walsh. *An Introduction to Stochastic Partial Differential Equations*. In: Hannequin, P.L. (eds) *École d'Été de Probabilités de Saint Flour XIV - 1984*. Lecture Notes in Mathematics, vol 1180. Springer, 1986.
- [30] R. Cont and P. Tankov. *Financial Modelling with Jump Processes*. Chapman & Hall/CRC Financial Mathematics Series. CRC Press LLC, 2003.
- [31] J. Mercer. Functions of positive and negative type, and their connection with the theory of integral equations. *Philos. T. Roy. Soc. A*, 209:415–446, May 1909.
- [32] R. Kress. *Linear Integral Equations*. Applied Mathematical Sciences 82. Springer, 1999.
- [33] I. Daubechies, M. Defrise, and C. De Mol. An iterative thresholding algorithm for linear inverse problems with a sparsity constraint. *Comm. Pure Appl. Math.*, 57:1413–1457, November 2004.
- [34] S.M. Zemyan. *The Classical Theory of Integral Equations A Concise Treatment*. Springer, 2012.
- [35] I. Daubechies. *Ten Lectures on Wavelets*. Philadelphia: SIAM, 1992.
- [36] G. Beylkin and N. Saito. Wavelets, their autocorrelation functions, and multiresolution representations of signals. In David P. Casasent, editor, *Intelligent Robots and Computer Vision XI: Biological, Neural Net, and 3D Methods*, volume 1826, pages 39–50. International Society for Optics and Photonics, SPIE, 1992.
- [37] R. Killick, M.I. Knight, G.P. Nason, and I.A. Eckley. The local partial autocorrelation function and some applications. *Elec. J. Stat.*, 14(2):3268 – 3314, 2020.
- [38] P.J. Diggle and I. al Wasel. Spectral analysis of replicated biomedical time series. *J. R. Statist. Soc. C*, 46(1):31–71, 1997.
- [39] J. Embleton, M.I. Knight, and H. Ombao. Multiscale spectral modelling for nonstationary time series within an ordered multiple-trial experiment. *The Annals of Applied Statistics*, 16(4):2774 – 2803, 2022.
- [40] D.L. Donoho and I.M. Johnstone. Ideal spatial adaption via wavelet shrinkage. *Biometrika*, 81:425–455, 1994.
- [41] M.H. Neumann and R. von Sachs. Wavelet thresholding: Beyond the gaussian i.i.d. situation. pages 301–329, 1995.
- [42] R. von Sachs and K. Schneider. Wavelet smoothing of evolutionary spectra by nonlinear thresholding. *Applied and Computational Harmonic Analysis*, 3(3):268–282, 1996.
- [43] H. Gao. *Spectral density estimation via wavelet shrinkage*. PhD thesis, U. C. Berkeley, 1993.
- [44] Michael H. Neumann. Spectral density estimation via non-linear wavelet methods for stationary non-gaussian time series. *Journal of Time Series Analysis*, 17(6):601–633, 1996.
- [45] R. von Sachs, G.P. Nason, and G. Kroisandt. Adaptive estimation of the evolutionary wavelet spectrum. *University of Kaiserslautern, Germany, and University of Bristol, UK*, 1997.
- [46] P. Fryzlewicz and V. Delouille. A data-driven haar-fisz transform for multiscale variance stabilization. In *IEEE/SP 13th Workshop on Statistical Signal Processing, 2005*, pages 539–544, 2005.
- [47] P. Fryzlewicz and G.P. Nason. Haar–Fisz Estimation of Evolutionary Wavelet Spectra. *Journal of the Royal Statistical Society Series B: Statistical Methodology*, 68(4):611–634, 07 2006.
- [48] O. Walch, Y. Huang, D. Forger, and C. Goldstein. Sleep stage prediction with raw acceleration and photoplethysmography heart rate data derived from a consumer wearable device. *Sleep*, 42(12), 08 2019. zsz180.
- [49] O. Walch. Motion and heart rate from a wrist-worn wearable and labeled sleep from polysomnography. *PhysioNet*, Oct 2019.
- [50] J. Buesco and A.C. Paixao. Eigenvalue distribution of mercer-like kernels. *Math. Nachr.*, 280:935–1218, June 2007.
- [51] T. Hastie, R. Tibshirani, and J. Friedman. *The Elements of Statistical Learning*. Springer, 2009.

A - Background Materials

This section reviews some of the relevant background materials in more detail beginning with locally stationary wavelet processes in discrete time, followed by Lévy processes and bases and concludes with some useful methods for solving linear integral equations.

6.1 Review of Locally Stationary Wavelet Processes in Discrete Time

Locally stationary wavelet processes [9, 18] are time series models that have found applications in various domains, including finance [6], economics [19], aliasing detection [20, 21], biology [22] and energy [24, 25]. They are constructed from discrete wavelets as follows.

Definition 14. (Discrete Wavelets). [9] Let $\{g_k\}_{k \in \mathbb{Z}}$ and $\{h_k\}_{k \in \mathbb{Z}}$ be the high and low-pass quadrature mirror filters used in the construction of the Daubechies [35] compactly supported orthogonal continuous wavelets. Let N_h be the number of non-zero elements of $\{h_k\}_{k \in \mathbb{Z}}$ and $N_j = (2^j - 1)(N_h - 1) + 1$ for scales $j \in \mathbb{N}$. Then the discrete wavelets $\psi_j = (\psi_{j,0}, \psi_{j,1}, \dots, \psi_{j,N_j-1})$ are vectors of length N_j obtained using the formulae

$$\psi_{1,n} = \sum_k g_{n-2k} \delta_{0,k} = g_n, \quad n = 0, \dots, N_1 - 1, \quad (83)$$

$$\psi_{j+1,n} = \sum_k h_{n-2k} \psi_{j,k}, \quad n = 0, \dots, N_{j+1} - 1, \quad (84)$$

where $\delta_{0,k}$ denotes the Kronecker delta.

The locally stationary wavelet processes can then be defined as follows.

Definition 15. (Locally Stationary Wavelet Process). [9] A locally stationary wavelet process is a sequence of stochastic processes $\{X_{t,T}\}_{t=0,\dots,T-1}$ ($T = 2^j$, for some $j \in \mathbb{N}$) having the following representation in the mean square sense:

$$X_{t,T} = \sum_{j=1}^{\infty} \sum_{k=-\infty}^{\infty} w_{j,k;T} \psi_{j,k-t} \xi_{j,k}, \quad (85)$$

where $\{w_{j,k;T}\}_{j \in \mathbb{N}, k \in \mathbb{Z}}$ is a set of amplitudes, $\{\psi_{j,k-t}\}_{j \in \mathbb{N}, k \in \mathbb{Z}}$ are discrete wavelets and $\{\xi_{j,k}\}_{j \in \mathbb{N}, k \in \mathbb{Z}}$ is a set of random variables with zero mean and unit variance. Furthermore, for each $j \in \mathbb{N}$ there exists a Lipschitz continuous function $W_j : (0, 1) \mapsto \mathbb{R}$ such that:

- (a) $\sum_{j=1}^{\infty} |W_j(z)|^2 < \infty$ uniformly in $z \in (0, 1)$;
- (b) the Lipschitz constants, L_j , are uniformly bounded in j and $\sum_{j=1}^{\infty} 2^j L_j < \infty$;
- (c) there exist constants $\{C_j\}_{j \in \mathbb{N}}$ such that for each T ,

$$\sup_k |w_{j,k;T} - W_j(k/T)| \leq C_j/T, \quad (86)$$

where for each j the supremum is over $k = 0, 1, \dots, T - 1$ and $\{C_j\}_{j \in \mathbb{N}}$ is such that $\sum_{j=1}^{\infty} C_j < \infty$.

The functions W_j are employed in LSW (locally stationary wavelet) models using re-scaled time, which involves scaling the process from \mathbb{N} to the unit interval $(0, 1)$. This concept, introduced by [8], is commonly employed when working with locally stationary processes. Within this framework, the limit $T \rightarrow \infty$ is interpreted as an increasing amount of information becoming available regarding the local characteristics of the process. We now present spectral quantities:

Definition 16. (Evolutionary Wavelet Spectrum). [9] The evolutionary wavelet spectrum of the locally stationary wavelet process $\{X_{t,T}\}_{t=0,\dots,T-1}$ is defined as

$$S_j(z) = |W_j(z)|^2, \quad j \in \mathbb{N}, \quad z \in (0, 1) \quad (87)$$

with respect to $\{\psi_{j,k}\}$.

The evolutionary wavelet spectrum provides a time-scale decomposition of the contribution to the variance of the process $X_{t,T}$. Note $S_j(z)$ is approximately equivalent to the variance of the process integrated over frequency band $[2^{-j}\pi, 2^{1-j}\pi]$, although the exact frequency band depends on the choice of wavelet. [20]

One of the fundamental concepts in the study of time series is that of the autocovariance of a process. Fortunately, for locally stationary wavelet processes, the autocovariance can be expressed in terms of the underlying wavelets and the evolutionary wavelet spectrum. This representation mirrors that of the autocovariance of a stationary time series in the Fourier domain,

$$c(\tau) = \int_{-\infty}^{\infty} \exp(i\omega\tau) dS(\omega). \quad (88)$$

and necessitates autocorrelation wavelets defined next.

Definition 17. (Autocorrelation Wavelets). [9] Let $j, \ell \in \mathbb{N}$ and $\tau \in \mathbb{Z}$. The autocorrelation wavelets are given by

$$\Psi_j(\tau) = \sum_k \psi_{j,k} \psi_{j,k-\tau}, \quad (89)$$

and the corresponding inner product operator is defined as

$$A_{j,\ell} = \sum_{\tau} \Psi_j(\tau) \Psi_{\ell}(\tau). \quad (90)$$

Definition 18. (Local Autocovariance). [9] The local autocovariance of the locally stationary wavelet process $\{X_{t,T}\}_{t=0,\dots,T-1}$ is defined as

$$c(z, \tau) = \sum_{j=1}^{\infty} S_j(z) \Psi_j(\tau), \quad \tau \in \mathbb{Z}, \quad z \in (0, 1). \quad (91)$$

The local autocovariance $c(z, \tau)$ is the limit of the autocovariance $c_T(z, \tau)$ of the process X_T as $T \rightarrow \infty$. [9].

We conclude this section with the definition of the raw wavelet periodogram, which is a biased estimator of the evolutionary wavelet spectrum. To obtain an unbiased estimator of the evolutionary wavelet spectrum, it is necessary to correct the raw periodogram using the inner product operator defined in 90, see [9] for further information.

Definition 19. (Raw Wavelet Periodogram). [9] The raw wavelet periodogram of the locally stationary wavelet process $\{X_{t,T}\}_{t=0,\dots,T-1}$ is defined as

$$I_{\ell,m} = d_{\ell,m}^2, \quad \ell \in \mathbb{N}, \quad m \in \mathbb{Z}, \quad (92)$$

where $\{d_{\ell,m}\}$ are the non-decimated wavelet coefficients of $X_{t,T}$ given by

$$d_{\ell,m} = \sum_{t=0}^{T-1} X_{t,T} \psi_{\ell,m-t}, \quad \ell \in \mathbb{N}, \quad m \in \mathbb{Z}. \quad (93)$$

6.2 Review of Lévy Processes

We now provide a brief overview of Lévy processes and bases, which play a crucial role in the definition of locally stationary wavelet processes in continuous time. The contents of this section draw heavily from [26, 27, 28, 29, 30]. In the following discussion, we take $(\Omega, \mathcal{F}, \mathbb{P})$ to be the underlying probability space, $(S, \mathcal{B}(S))$ to be a Borel space and denote the bounded Borel sets of $\mathcal{B}(S)$ by $\mathcal{B}_b(S)$. Definitions 20 through to Proposition 7 provide the basic underlying machinery for the construction of our continuous time locally stationary wavelet processes.

Definition 20. (Infinite Divisibility). [26, 28] Let X be a real-valued random variable. Then X is infinitely divisible if, for all $n \in \mathbb{N}$, there exist i.i.d. random variables $Y_1^{(n)}, \dots, Y_n^{(n)}$ such that $X \stackrel{d}{=} Y_1^{(n)} + \dots + Y_n^{(n)}$, where $\stackrel{d}{=}$ denotes equivalence in distribution.

Definition 21. (Lévy Process). [26, 30] A real-valued stochastic process $L = \{L(t)\}_{t>0}$ on $(\Omega, \mathcal{F}, \mathbb{P})$ is called a Lévy process if it exhibits the following properties:

- (a) $L(0) = 0$ almost surely,
- (b) L has independent increments: for any $n \in \mathbb{N}$ and any sequence of times $t_0 < t_1 < \dots < t_n$, the random variables $L(t_0), L(t_1) - L(t_0), \dots, L(t_n) - L(t_{n-1})$ are independent,
- (c) L has stationary increments: the law of $L(t+s) - L(t)$ does not depend on t ,
- (d) L is continuous in probability: $\forall \varepsilon > 0, \lim_{h \rightarrow 0} \mathbb{P}(|L(t+h) - L(t)| \geq \varepsilon) = 0$,

(e) L has càdlàg paths.

Theorem 6. (Lévy-Khintchine). [28, 26] Let X be an \mathbb{R}^n -valued random variable. Then X is infinitely divisible if there exists a vector $b \in \mathbb{R}^n$, a positive definite symmetric $n \times n$ matrix A and a Lévy measure ν on $\mathbb{R}^n \setminus \{0\}$, i.e. a measure satisfying $\int_{\mathbb{R}^n \setminus \{0\}} \max(|y|^2, 1) \nu(dy) < \infty$, such that, for all $u \in \mathbb{R}^n$,

$$\begin{aligned} \phi_X(u) &= \mathbb{E}(\exp(i\langle u, X \rangle)) \\ &= \exp i\langle b, u \rangle - \frac{1}{2} \langle u, Au \rangle + \int_{\mathbb{R}^n \setminus \{0\}} \left(e^{i\langle u, y \rangle} - 1 - i\langle u, y \rangle \mathbb{1}_{B_1(0)}(y) \right) \nu(dy), \end{aligned} \quad (94)$$

where $B_1(0)$ is the open ball of radius 1 centred at 0 and $\langle \cdot, \cdot \rangle$ denotes the inner product in \mathbb{R}^d . Conversely, any mapping of this form is the characteristic function of an infinitely divisible random variable on \mathbb{R}^n .

Since every Lévy process is infinitely divisible, its characteristic function also takes the above form. Therefore, a Lévy process can be seen as a Brownian motion with drift b interspersed with jumps of arbitrary size [28].

Definition 22. (Random Measure). [28, 26] A random measure M is a collection of real-valued random variables $\{M(A) : A \in \mathcal{B}_b(S)\}$ such that if A_1, A_2, \dots is a sequence of disjoint elements of $\mathcal{B}_b(S)$ satisfying $\bigcup_{j=1}^{\infty} A_j \in \mathcal{B}_b(S)$, then

$$M\left(\bigcup_{j=1}^{\infty} A_j\right) = \sum_{j=1}^{\infty} M(A_j), \quad (95)$$

where the right hand side converges almost surely (a.s.).

Definition 23. (Stationarity). [26] A random measure M is said to be stationary if for all $s \in S$ and any finite collection A_1, A_2, \dots, A_n of elements of $\mathcal{B}_b(S)$, the random vector $\{M(A_1 + s), M(A_2 + s), \dots, M(A_n + s)\}$ has the same law as $\{M(A_1), M(A_2), \dots, M(A_n)\}$.

Definition 24. (Lévy Basis). [26] A real valued Lévy basis on S is a collection $\{L(A) : A \in \mathcal{B}_b(S)\}$ of random variables satisfying the following properties:

(a) If A and B are disjoint subsets in $\mathcal{B}_b(S)$, then

$$L(A \cup B) = L(A) + L(B), \quad \text{a.s.} \quad (96)$$

(b) If A and B are disjoint subsets in $\mathcal{B}_b(S)$, then $L(A)$ and $L(B)$ are independent,

(c) The law of $L(A)$ is infinitely divisible for all $A \in \mathcal{B}_b(S)$.

Equivalently, we could define a Lévy basis L as an independently scattered (i.e. if A_1, A_2, \dots is a sequence of disjoint elements of $\mathcal{B}_b(S)$, then the random variables $M(A_1), M(A_2), \dots$ are independent), infinitely divisible random measure. See [26] for a proof of the equivalence between the two definitions.

Proposition 6. [26] Let L be a Lévy basis and $u \in \mathbb{R}$. Then for all $A \in \mathcal{B}_b(S)$,

$$\phi_{L(A)}(u) = \mathbb{E}[\exp\{iuL(A)\}] \quad (97)$$

$$= \exp \left\{ iu \xi^*(A) - \frac{1}{2} u^2 a^*(A) + \int_{\mathbb{R}} \left(e^{iux} - 1 - iux \mathbb{1}_{[-1,1]}(x) \right) n(dx, A) \right\} \quad (98)$$

where ξ^* is a signed measure on $\mathcal{B}_b(S)$, a^* is a measure on $\mathcal{B}_b(S)$ and $n(\cdot, \cdot)$ is the generalised Lévy measure.

Since the law of $L(A)$ for all $A \in \mathcal{B}_b(S)$ it is infinitely divisible, it is not surprising that it has a Lévy-Khintchine representation.

Definition 25. (Homogeneous Lévy Basis). [26] Let L denote a Lévy basis on $(\mathbb{R}^n, \mathcal{B}(\mathbb{R}^n))$. If ξ^* , a^* , $n(dx, \cdot)$, as defined in Proposition 6 are all absolutely continuous with respect to the Lebesgue measure and their Radon-Nikodym derivatives do not depend on $z \in S$, the L is a homogeneous Lévy basis.

Proposition 7. [26] Let L be a Lévy basis on $(\mathbb{R}^n, \mathcal{B}(\mathbb{R}^n))$. Then L is homogeneous if and only if it is stationary.

When defining continuous time locally stationary wavelet processes, we restrict our attention to homogeneous Lévy bases as the above proposition makes the concepts of homogeneity and stationarity synonymous. This is a desirable property, as we would like to control the non-stationarity of the process entirely through the deterministic amplitude functions of the process. More on this in Section 3.

Example 2 (Homogeneous Gaussian Lévy Basis). [26] Let G be a Lévy basis. If $G(A) \sim \mathcal{N}(\mu \text{Leb}(A), \sigma^2 \text{Leb}(A))$ for all $A \in \mathcal{B}(\mathbb{R}^n)$, for some $\mu \in \mathbb{R}$ and $\sigma \in \mathbb{R}^+$, then G is a homogeneous Gaussian Lévy basis. Gaussian Lévy bases are equivalent to the concept of white noise as defined in [29].

If L is a homogeneous Lévy basis on $(\mathbb{R}, \mathcal{B}(\mathbb{R}))$, then the process $(L_t)_{t \geq 0}$ with $L_t = L([0, t])$ is a Lévy process. Conversely, given a Lévy process $(L_t)_{t \geq 0}$, we can obtain a Lévy basis L by setting $L((s, t]) = L_t - L_s$. It is easy to see a similar connection between a homogeneous Gaussian Lévy basis and Brownian motion. [26]

6.3 Review of Linear Integral Equations and Regularisation Methods

Lastly, we review the relevant concepts on linear integral equations and regularisation methods. Although not strictly necessary for defining locally stationary wavelet process in continuous time, these tools will be useful when we wish to obtain an estimate of the evolutionary wavelet spectrum. The material presented in this section draws from [32, 33, 31, 34]. We denote the adjoint of a linear operator, T , by T^\dagger , its eigenvalues and eigenfunctions by λ_n and φ_n respectively, and the null space of T by $N(T)$.

Definition 26. (Integral Operator) [32] Let $S \subset \mathbb{R}^n$, $K : S \times S \mapsto \mathbb{R}$ be a continuous function and $h \in L^2(S)$. Then the linear operator $T : L^2(S) \mapsto L^2(S)$ defined by

$$(Th)(x) = \int_S K(x, y)h(y) dy, \quad x \in S, \quad (99)$$

is called an integral operator with continuous kernel K . Integral operators are compact and bounded.

We focus on linear integral equations of the first kind, given by

$$Th = f \quad (100)$$

where $f \in L^2(S)$ and the integral operator T are known, and $h \in L^2(S)$ unknown. However, compact linear operators do not possess a bounded inverse, which can lead to problems when attempting to invert the above equation in order to obtain h .

When T is a self-adjoint compact linear operator on a Hilbert space, T has at most countably many different eigenvalues λ_n accumulating at zero. Denoting the orthogonal projections onto the eigenspaces by P_n and assuming that the sequence of non-zero eigenvalues is ordered such that $|\lambda_1| \geq |\lambda_2| \geq \dots$, we have

$$T = \sum_{n=1}^{\infty} \lambda_n P_n \quad (101)$$

in the sense of norm convergence. Under certain conditions, Mercer's theorem [31] also gives us a decomposition of the kernel:

Theorem 7. (Mercer's Theorem) [31] [50] Let T be a linear integral operator defined by

$$(Th)(x) = \int_S K(x, y)h(y) dy \quad (102)$$

where K is a continuous symmetric non-negative definite kernel. Then the kernel K can be expanded in terms of the eigenvalues λ_n and eigenfunctions φ_n of T as

$$K(x, y) = \sum_{n=1}^{\infty} \lambda_n \varphi_n(x) \varphi_n(y), \quad (103)$$

where the convergence is absolute and uniform. The non-negative definite kernel implies non-negative eigenvalues, which decay at a rate of $O(n^{-1})$.

When T is a self-adjoint linear operator, we can use the above to obtain a solution to (100) of the form

$$h = \sum_{n=1}^{\infty} \frac{1}{\lambda_n} \langle f, \varphi_n \rangle \varphi_n, \quad (104)$$

provided that $f \in N(T)^\perp$ (f belongs to the orthogonal complement of the null space of T) and

$$\sum_{n=1}^{\infty} \frac{1}{\lambda_n^2} |\langle f, \varphi_n \rangle|^2 < \infty. \quad (105)$$

If T was not self-adjoint, we have a similar expression in terms of its singular value decomposition. [32]

Typically one also encounters noise contamination of the form $Th = f + \varepsilon$, where g denotes the true function and ε the noise, whose effects on the solution can be amplified due to the unboundedness of T^{-1} . This is particularly pronounced for smaller eigenvalues. To address this issue, a simple often used regularisation approach is the spectral cut-off method, which replaces the solution with

$$h_\mu = \sum_{\lambda_n^2 > \mu} \frac{1}{\lambda_n} \langle f, \varphi_n \rangle \varphi_n, \quad (106)$$

for some $\mu > 0$. Alternatively, (100) can be reformulated as a minimisation problem, with the aim of minimising the discrepancy:

$$\Delta h = \|Th - f\|^2. \quad (107)$$

A pseudo-solution of the form $\tilde{h} = (T^\dagger T)^{-1} T^\dagger f$ can be obtained, assuming that T has a trivial null space ($N(T) = \{0\}$). However, the unboundedness of T^{-1} and the presence of noise can lead to difficulties. To attempt to deal with this problem, Tikhonov regularisation, also known as ridge regression [51], is commonly employed. It involves minimising the constrained discrepancy

$$\Delta h = \|Th - f\|^2 + \mu \|h\|^2, \quad (108)$$

for some $\mu > 0$, in order to obtain a solution of the form

$$h_\mu = (T^\dagger T + \mu I)^{-1} T^\dagger f, \quad (109)$$

essentially penalising solutions with large norms. When T is self-adjoint, the above can be written in the form

$$h_\mu = \sum_{n=1}^{\infty} \frac{\lambda_n}{\lambda_n^2 + \mu} \langle f, \varphi_n \rangle \varphi_n \quad (110)$$

instead.

In [33], the authors propose to minimise

$$\Phi_{\mu,p}(h) = \|Th - f\|^2 + \sum_{\gamma \in \Gamma} \mu_\gamma |\langle h, e_\gamma \rangle|^p, \quad (111)$$

where $\{e_\gamma\}_{\gamma \in \Gamma}$ is an orthogonal basis of the Hilbert space H , $\boldsymbol{\mu} = \{\mu_\gamma\}_{\gamma \in \Gamma}$ is a vector of weights, which act as regularisation parameters, and $1 \leq p \leq 2$. The solution can be obtained via an iterative scheme given by

$$h^n = \mathbf{Shrink}_{\boldsymbol{\mu},1} \{h^{n-1} + T^\dagger (f - Th^{n-1})\}, \quad (112)$$

where

$$\mathbf{Shrink}_{\boldsymbol{\mu},1}(h) = \sum_{\gamma} \mathit{Shrink}_{\mu_\gamma,1}(\langle h, e_\gamma \rangle) e_\gamma \quad (113)$$

and

$$\mathit{Shrink}_{\mu_\gamma,1}(x) = \begin{cases} x - \mu_\gamma/2, & \text{if } x \geq \mu_\gamma/2, \\ 0, & \text{if } |x| < \mu_\gamma/2, \\ x + \mu_\gamma/2, & \text{if } x \leq -\mu_\gamma/2. \end{cases} \quad (114)$$

We use the notation $\mathbf{Shrink}_{\boldsymbol{\mu},1}$ when applying the shrink operation to vectors and $\mathit{Shrink}_{\mu_\gamma,1}$ when applying it to numbers. The authors also discuss an extension of this algorithm for cases in which one want to penalise the positive and negative coefficients need to be penalised differently. To do so, one would replace each μ_γ with the positive weights $(\mu_\gamma^+, \mu_\gamma^-)$ and (114) with

$$\mathit{Shrink}_{\mu_\gamma,1}(x) = \begin{cases} x - \mu_\gamma^+/2, & \text{if } x \geq \mu_\gamma^+/2, \\ 0, & \text{if } -\mu_\gamma^-/2 < x < \mu_\gamma^+/2, \\ x + \mu_\gamma^-/2, & \text{if } x \leq -\mu_\gamma^-/2. \end{cases} \quad (115)$$

We conclude this section by stating the two main results of [33].

Theorem 8. Consider the iterative scheme defined by (112) for $n = 1, 2, \dots$, with arbitrarily chosen $h^0 \in H$. Then h^n converges strongly to the unique minimiser of $\Phi_{\boldsymbol{\mu},p}$.

Theorem 9. If $\boldsymbol{\mu} = \boldsymbol{\mu}(\varepsilon)$, where ε denotes the noise level, satisfies

$$\lim_{\varepsilon \rightarrow 0} \boldsymbol{\mu}(\varepsilon) = 0 \quad \text{and} \quad \lim_{\varepsilon \rightarrow 0} \varepsilon^2 / \boldsymbol{\mu}(\varepsilon) = 0, \quad (116)$$

then

$$\lim_{\varepsilon \rightarrow 0} \left[\sup_{\|f - Th\| \leq \varepsilon} \|h_{\boldsymbol{\mu}(\varepsilon)}^* - h\| \right] = 0, \quad (117)$$

for any $h \in H$, where $h_{\boldsymbol{\mu}(\varepsilon)}^*$ denotes the unique minimiser of $\Phi_{\boldsymbol{\mu},p}$.

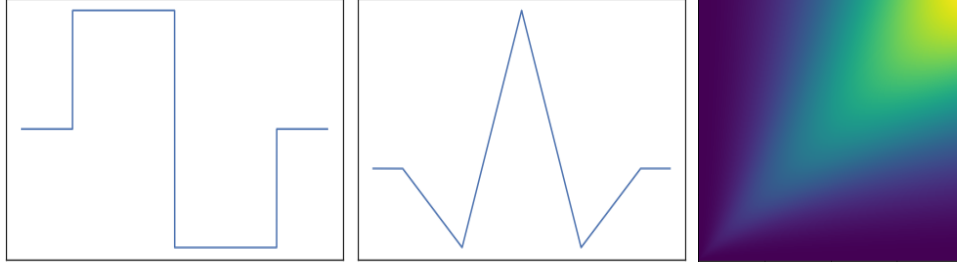


Figure 7: Haar wavelet (left), autocorrelation wavelet (centre) and inner product kernel (right).

B - Some Autocorrelation Wavelets and Inner Product Kernels

In this short section we provide some examples of continuous wavelets and their corresponding autocovariance wavelets and inner product kernels.

Haar Wavelet

We begin by presenting the most common and simplest example of a wavelet the Haar wavelet. Its definition can be found in the main text.

Proposition 8. (Autocorrelation Wavelet). Let $u \in \mathbb{R}^+$ and $\tau \in \mathbb{R}$. Then the Haar autocorrelation wavelet is given by

$$\Psi_H(u, \tau) = \begin{cases} 1 - 3|\tau|/u, & 0 < |\tau| \leq u/2, \\ |\tau|/u - 1, & u/2 < |\tau| \leq u, \\ 0, & \text{otherwise.} \end{cases} \quad (118)$$

Proposition 9. (Inner Product Kernel). Let $u, x \in \mathbb{R}^+$. The the Haar inner product kernel is given by

$$A_H(u, x) = \begin{cases} \frac{x^2}{2u}, & 0 < x \leq u/2, \\ 2x - u + \frac{u^2}{6x} - \frac{5x^2}{6u}, & u/2 < x \leq u, \\ 2u - x + \frac{x^2}{6u} - \frac{5u^2}{6x}, & u < x \leq 2u, \\ \frac{u^2}{2x}, & x \geq 2u. \end{cases} \quad (119)$$

Ricker Wavelet

The second wavelet we present is the Ricker wavelet, which is defined as the negative normalised second derivative of the Gaussian function. In terms of width, it can be considered an intermediate between the Haar and Shannon wavelets. While it does not have compact support, its tails decay rapidly to zero, similar to a Gaussian probability density function.

Definition 27. (Ricker Wavelet). Let $u \in \mathbb{R}^+$ and $x \in \mathbb{R}$. The the Ricker wavelet is defined as

$$\psi_R(u, x) = \frac{2}{\pi^{1/4}\sqrt{3u}} \left(1 - \frac{x^2}{u^2}\right) e^{-\frac{x^2}{2u^2}}. \quad (120)$$

Proposition 10. (Autocorrelation Wavelet). Let $u \in \mathbb{R}^+$ and $\tau \in \mathbb{R}$. Then the Ricker autocorrelation wavelet is given by

$$\Psi_R(u, \tau) = \left(1 + \frac{\tau^4}{12u^4} - \frac{\tau^2}{u^2}\right) e^{-\frac{\tau^2}{4u^2}}. \quad (121)$$

Proposition 11. (Inner Product Kernel). Let $u, x \in \mathbb{R}^+$. The the Ricker inner product kernel is given by

$$A_R(u, x) = \frac{70\sqrt{\pi} u^5 x^5}{3(u^2 + x^2)^{\frac{9}{2}}}. \quad (122)$$

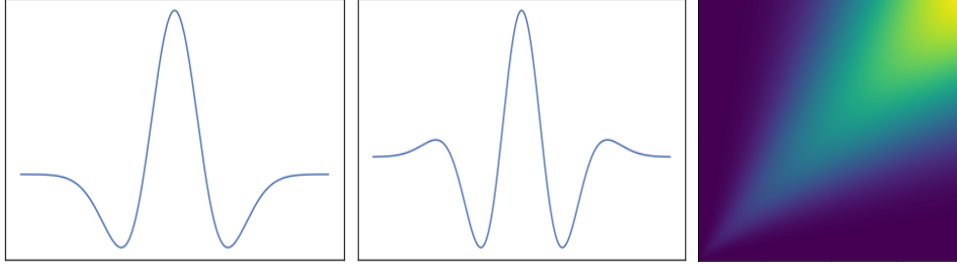


Figure 8: Ricker wavelet (left), autocorrelation wavelet (centre) and inner product kernel (right).

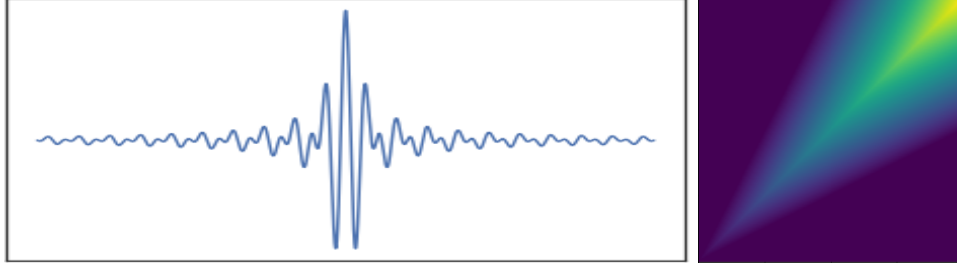


Figure 9: Shannon wavelet and autocorrelation wavelet (left - one is simply a rescaled version of the other) and inner product kernel (right).

Shannon Wavelet

The final wavelet family we present is the Shannon wavelet family, which can easily be considered the widest of the three.

Definition 28. (Shannon Wavelet). Let $u \in \mathbb{R}^+$ and $x \in \mathbb{R}$. The the Shannon wavelet is defined as

$$\psi_S(u, x) = \sqrt{u} \frac{1}{\pi x} \left[\sin\left(\frac{2\pi x}{u}\right) - \sin\left(\frac{\pi x}{u}\right) \right]. \quad (123)$$

Its Fourier transform is given by

$$\hat{\psi}_S(u, \omega) = \sqrt{u} \left(\mathbb{1}_{[-\frac{2\pi}{u}, -\frac{\pi}{u}]}(\omega) + \mathbb{1}_{[\frac{\pi}{u}, \frac{2\pi}{u}]}(\omega) \right). \quad (124)$$

Proposition 12. (Autocorrelation Wavelet). Let $u \in \mathbb{R}^+$ and $\tau \in \mathbb{R}$. Then the Shannon autocorrelation wavelet is given by

$$\Psi_S(u, \tau) = \sqrt{u} \psi_S(u, \tau). \quad (125)$$

Proposition 13. (Inner Product Kernel). Let $u, x \in \mathbb{R}^+$. The the Shannon inner product kernel is given by

$$A_S(u, x) = \begin{cases} 2x - u, & u/2 \leq x \leq u, \\ 2u - x, & u < x \leq 2u, \\ 0, & \text{otherwise.} \end{cases} \quad (126)$$

C - A Comparison of the Local and Standard Autocovariance Functions

Recall that, for $t, \tau \in \mathbb{R}$, the local autocovariance and the standard autocovariance functions are given by

$$c(t, \tau) = \int_0^\infty S(u, t) \Psi(u, \tau) du \quad (127)$$

and

$$c_X(t, \tau) = \int_0^\infty \int_{-\infty}^\infty S(u, t+v) \psi(u, v) \psi(u, v-\tau) dv du, \quad (128)$$

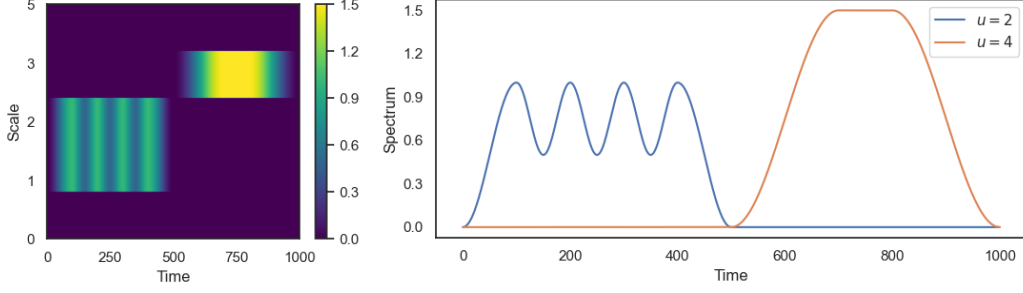


Figure 10: From left to right: the full evolutionary wavelet spectrum and the evolutionary wavelet spectrum at scales $u = 2$ and $u = 4$.

respectively, as defined in Section 3. Proposition 1 established a global bound on the discrepancy between (127) and (128). One can also obtain a bound which depends on the lag τ and is given by

$$|c_X(t, \tau) - c(t, \tau)| \leq \gamma \left| \int_0^\infty uK(u)\Psi(u, \tau) du \right|, \quad (129)$$

as derived in the proof of Proposition 1. From this bound we see that the discrepancy between the two decreases to zero as τ increases.

We now analyse the difference between the two quantities through the use of a simple example. The evolutionary wavelet spectrum we consider is given by

$$S(u, t) = \begin{cases} (\cos[\pi(t - 100)/100] + 1) / 2, & \text{for } 0 \leq t \leq 100, \\ \cos(\pi t/50)/4 + 3/4, & \text{for } 100 < t \leq 400, \\ (\cos(\pi t/100) + 1) / 2, & \text{for } 400 < t \leq 500, \\ 0, & \text{otherwise,} \end{cases} \quad (130)$$

for $1 \leq u \leq 3$,

$$S(u, t) = \begin{cases} 3(\cos[\pi(t + 100)/200] + 1) / 4, & \text{for } 500 < t \leq 700, \\ 3/2, & \text{for } 700 < t \leq 800, \\ 3(\cos(\pi t/200) + 1) / 4, & \text{for } 800 < t \leq 1000 \\ 0, & \text{otherwise,} \end{cases} \quad (131)$$

for $3 < u \leq 4$ and zero otherwise. This is displayed in Figure 10, as well as a plot of the spectrum at scales $u = 2$ and $u = 4$. The evolutionary wavelet spectrum displays a wide variety of different behaviours. To compare (127) and (128) over a wider range of scales, we also redefine the same spectrum but with the scales replaced by factors of 4 and 10. We take the underlying wavelets to be Ricker wavelets. There is no particular reason for this choice and this comparison can easily be repeated for other wavelets as well. Although in theory $\psi_R(x) > 0$ for all $x \in \mathbb{R}$, the tails decay rapidly enough that we can assume $\psi_R(x) \approx 0$ for $x \notin (-4, 4)$.

As discussed in the main text, the local autocovariance at each time $t \in \mathbb{R}$ is computed under the assumption that the spectrum remains constant at $S(u, t)$ over the domain of the underlying wavelet. Figure 11 provides further insight into this. On the left we depict the Ricker wavelet for different values of τ , highlighting that only the region over which they overlap contributes to the autocovariance of the process, this being maximal at $\tau = 0$. This also offers a visual interpretation to the bound in (129). On the right, we display a portion of the spectrum. Horizontal lines represent the value used in computing the local autocovariance for a range of scales u , with the width of this region increasing linearly with the scales.

We compute the local autocovariance and the standard autocovariance for the evolutionary wavelet spectra defined above and present the results in Figure 12. The two quantities are almost indistinguishable in all cases, with the two computed from the spectrum defined using the coarsest scales displaying the most significant difference, as anticipated. As illustrated in the right panel of Figure 11, the wavelet width at these scale covers a significant portion of the spectrum. However, this scenario is unrealistic in practice, as we expect the spectrum to vary at a much slower rate at such wide scales. Despite this, the two quantities remain nearly identical, suggesting that in practice the local autocovariance and the standard autocovariance are generally indistinguishable, as also implied by the theoretical properties.

The comparison conducted in this brief section carries over quite naturally when examining the difference between the expectation of the raw wavelet periodogram and its approximation, for which a bound was established in Theorem 1.

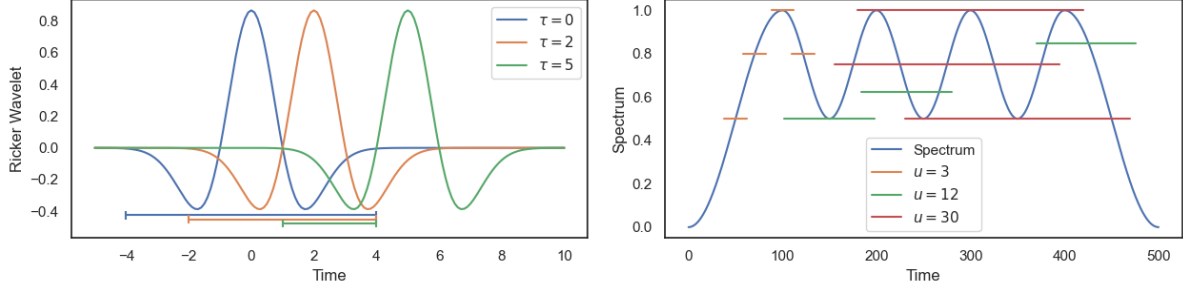


Figure 11: Left: the Ricker wavelet for scale $u = 1$, with shifts corresponding to different values of the lag τ . The horizontal lines below denote the region of overlap, which is the only non-zero contribution to the integral in (127) and (128). Right: the local autocovariance approximates the spectrum display with a constant in an interval of length at most equal to the width of the underlying wavelets. The horizontal lines display this for different scales u and times t .

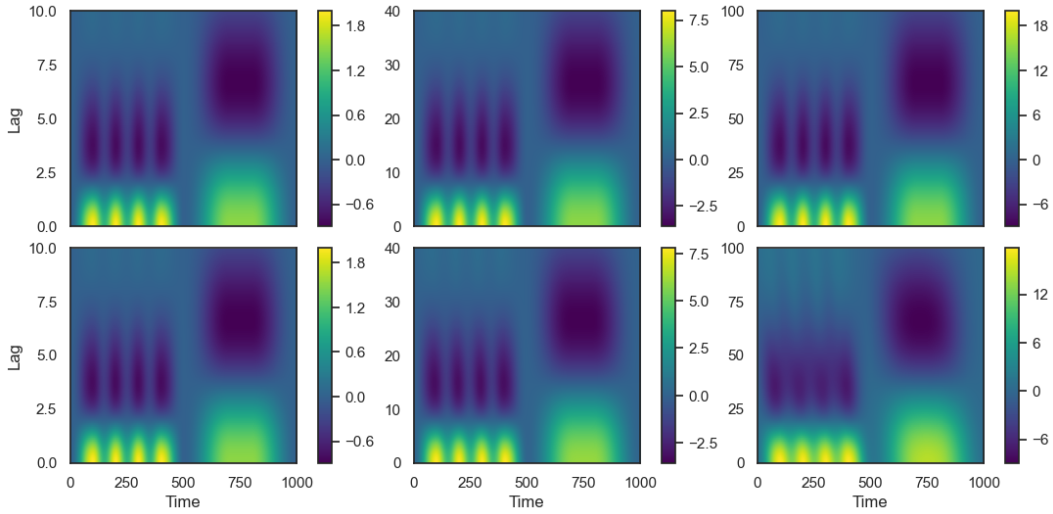


Figure 12: Top row: the local autocovariance. Bottom row: the standard autocovariance. From left to right: computations carried out using the evolutionary wavelet spectrum defined for scales $0 < u \leq 5$, $0 < u \leq 20$ and $0 < u \leq 100$.

Given that the spectrum is approximated in a similar manner as it is for the local autocovariance, we expect to obtain similar results.

D - Non-Stationary Haar Moving Average Spectrum

The functional form of the evolutionary wavelet spectrum for the example in Section 4.3 is given by

$$S(u, z) = \begin{cases} 1, & \text{for } z \in (0, 1/4] \quad \text{and } u \in (1/2, 3/2), \\ f(15 - 48z), & \text{for } z \in (1/4, 3/8) \quad \text{and } u \in (1/2, 3/2), \\ f(48z - 15), & \text{for } z \in (1/4, 3/8) \quad \text{and } u \in (3/2, 5/2), \\ 1, & \text{for } z \in [3/8, 5/8] \quad \text{and } u \in (3/2, 5/2), \\ f(33 - 48z), & \text{for } z \in (5/8, 3/4) \quad \text{and } u \in (3/2, 5/2), \\ f(48z - 33), & \text{for } z \in (5/8, 3/4) \quad \text{and } u \in (9/2, 11/2), \\ 1, & \text{for } z \in [3/4, 1) \quad \text{and } u \in (9/2, 11/2), \\ 0, & \text{otherwise,} \end{cases} \quad (132)$$

where

$$f(z) = \frac{1}{2} \tanh(z) + \frac{1}{2}. \quad (133)$$

E - Proofs

Proof of Proposition 1

The autocovariance of $X(t)$ can be written as

$$c_X(t, \tau) = \mathbb{E}[X(t)X(t + \tau)] \quad (134)$$

$$= \int_0^\infty \int_{-\infty}^\infty \int_0^\infty \int_{-\infty}^\infty W(u, v)W(x, y)\psi(u, v - t)\psi(x, y - t - \tau) du dv \quad (135)$$

$$= \int_0^\infty \int_{-\infty}^\infty |W(u, v)|^2 \psi(u, v - t)\psi(u, v - t - \tau) du dv \quad (136)$$

$$= \int_0^\infty \int_{-\infty}^\infty S(u, v + t)\psi(u, v)\psi(u, v - \tau) du dv, \quad (137)$$

where we used that $\mathbb{E}[L(du, dv)L(dx, dy)] = \delta(u - x)\delta(v - y) du dv dx dy$ and δ denotes the Dirac delta function. We also have that

$$c(t, \tau) = \int_0^\infty S(u, t)\Psi(u, \tau)du = \int_0^\infty S(u, t) \int_{-\infty}^\infty \psi(u, v)\psi(u, v - \tau) du dv, \quad (138)$$

and therefore

$$|c_X(t, \tau) - c(t, \tau)| = \left| \int_0^\infty \int_{-\infty}^\infty (S(u, v + t) - S(u, t)) \psi(u, v)\psi(u, v - \tau) du dv \right| \quad (139)$$

$$\leq \left| \int_0^\infty \int_{-\infty}^\infty |S(u, v + t) - S(u, t)| \psi(u, v)\psi(u, v - \tau) du dv \right| \quad (140)$$

$$\leq 2M \left| \int_0^\infty K(u) \int_{-\infty}^\infty |v| \psi(u, v)\psi(u, v - \tau) du dv \right| \quad (141)$$

$$\leq 2M\omega \left| \int_0^\infty uK(u) \int_{-\infty}^\infty \psi(u, v)\psi(u, v - \tau) du dv \right| \quad (142)$$

$$= 2M\omega \left| \int_0^\infty uK(u)\Psi(u, \tau) du \right| \quad (143)$$

$$\leq \gamma \int_0^\infty uK(u) du, \quad (144)$$

where in (141) we used that

$$|S(u, v + t) - S(u, t)| = ||W(u, v + t)|^2 - |W(u, t)|^2| \quad (145)$$

$$= |W(u, v + t) + W(u, t)| |W(u, v + t) - W(u, t)| \quad (146)$$

$$\leq 2MK(u)|v|, \quad (147)$$

for some $M \in \mathbb{R}^+$ such that $|W(u, v)| \leq M$ for all $u \in \mathbb{R}^+$ and $v \in \mathbb{R}$. The inequality in (142) follows from the fact that the integral grows linearly in u , where $\omega \in \mathbb{R}^+$ is a constant that depends on the width and decay rate of ψ . Since $|\Psi(u, \tau)| \leq 1$ for all $u \in \mathbb{R}^+$ and $\tau \in \mathbb{R}$, we obtain the inequality in (144), where we define $\gamma = 2M\omega$. \square

Proof of Proposition 2

(a) Follows from the definition.

(b) $\Psi(u, 0) = \|\psi\|^2 = 1$.

(c) We have that

$$\Psi(u, \tau) = \int_{-\infty}^\infty \psi(u, v)\psi(u, v - \tau)dv = \frac{1}{u} \int_{-\infty}^\infty \psi\left(\frac{v}{u}\right) \psi\left(\frac{v - \tau}{u}\right) dv \quad (148)$$

$$= \int_{-\infty}^\infty \psi(y) \psi\left(y - \frac{\tau}{u}\right) dy = \Psi\left(\frac{\tau}{u}\right), \quad (149)$$

where we made the substitution $v = uy$.

(d) We have that

$$\Psi(\tau) = \int_{-\infty}^{\infty} \psi(v)\psi(v-\tau)dv = (\psi * \psi)(\tau), \quad (150)$$

where $*$ denotes the convolution operator. Hence

$$\hat{\Psi}(\omega) = \mathcal{F}(\Psi)(\omega) = |\hat{\psi}(\omega)|^2. \quad (151)$$

Since, $\Psi(u, \tau) = \Psi\left(\frac{\tau}{u}\right)$, we have

$$\hat{\Psi}(u, \omega) = \mathcal{F}\left(\Psi\left(\frac{\cdot}{u}\right)\right)(\omega) = u\hat{\Psi}(u\omega) = u|\hat{\psi}(u\omega)|^2. \quad (152)$$

(e) We have

$$\int_{-\infty}^{\infty} \Psi(u, \tau)d\tau = \int_{-\infty}^{\infty} \int_{-\infty}^{\infty} \psi(u, v)\psi(u, v-\tau)dv d\tau \quad (153)$$

$$= \int_{-\infty}^{\infty} \psi(u, v) \int_{-\infty}^{\infty} \psi(u, v-\tau)d\tau dv = 0, \quad (154)$$

as the inner integral is zero. \square

Proof of Proposition 3

Continuity follows from the continuity of the autocovariance wavelets. Symmetry is clear from the definition. We now show that A is non-negative definite. Let $c_i, c_j \in \mathbb{R}$ and $x_i, x_j \in \mathbb{R}^+$ for $i, j = 1, \dots, n$. Then

$$\sum_{i=1}^n \sum_{j=1}^n c_i c_j A(x_i, x_j) = \int_{-\infty}^{\infty} \sum_{i=1}^n \sum_{j=1}^n c_i c_j \Psi(x_i, y) \Psi(x_j, y) dy \quad (155)$$

$$= \int_{-\infty}^{\infty} \left(\sum_{i=1}^n c_i \Psi(x_i, y) \right)^2 dy \geq 0. \quad (156)$$

For the final property, we have

$$A(bx, by) = \int_{-\infty}^{\infty} \Psi(bx, \tau) \Psi(by, \tau) d\tau \quad (157)$$

$$= \int_{-\infty}^{\infty} \Psi\left(\frac{\tau}{bx}\right) \Psi\left(\frac{\tau}{by}\right) d\tau \quad (158)$$

$$= \int_{-\infty}^{\infty} \Psi\left(x, \frac{\tau}{b}\right) \Psi\left(y, \frac{\tau}{b}\right) d\tau \quad (159)$$

$$= b \int_{-\infty}^{\infty} \Psi(x, t) \Psi(y, t) dt \quad (160)$$

$$= bA(x, y), \quad (161)$$

where we used (c) from Proposition 2. \square

Proof of Theorem 1

We have that

$$\beta(u, v) = \mathbb{E}[I(u, v)] = \mathbb{E}\left[\left(\int_{-\infty}^{\infty} X(t)\psi(u, t-v)dt\right)^2\right] \quad (162)$$

$$= \int_{-\infty}^{\infty} \int_{-\infty}^{\infty} \mathbb{E}[X(t)X(s)]\psi(u, t-v)\psi(u, s-v) dt ds \quad (163)$$

Now,

$$\mathbb{E}[X(t)X(s)] = \int_0^{\infty} \int_{-\infty}^{\infty} |W(x, y)|^2 \psi(x, y-t)\psi(x, y-s) dx dy, \quad (164)$$

where we used the fact that $\mathbb{E}[L(dx, dy)L(d\eta, d\xi)] = \delta(\eta - x)\delta(\xi - y) d\eta d\xi dx dy$ and δ denotes the Dirac delta function. Hence,

$$\beta(u, v) = \int_{-\infty}^{\infty} \int_{-\infty}^{\infty} \int_0^{\infty} \int_{-\infty}^{\infty} S(x, y) \psi(x, y - t) \psi(x, y - s) \psi(u, t - v) \psi(u, s - v) dy dx dt ds \quad (165)$$

$$= \int_{-\infty}^{\infty} \int_{-\infty}^{\infty} \int_0^{\infty} \int_{-\infty}^{\infty} S(x, y + v) \psi(x, y - t) \psi(x, y - s) \psi(u, t) \psi(u, s) dy dx dt ds \quad (166)$$

$$= \int_0^{\infty} \int_{-\infty}^{\infty} S(x, y + v) \left(\int_{-\infty}^{\infty} \psi(x, y - t) \psi(u, t) dt \right)^2 dy dx, \quad (167)$$

where in (166) we made the substitution $y \mapsto y + v$ followed by $t - v \mapsto t$ and $s - v \mapsto s$. Now,

$$\int_0^{\infty} S(x, v) A(u, x) dx = \int_0^{\infty} S(x, v) \int_{-\infty}^{\infty} \Psi(x, \eta) \Psi(u, \eta) d\eta dx \quad (168)$$

$$= \int_0^{\infty} S(x, v) \int_{-\infty}^{\infty} \int_{-\infty}^{\infty} \Psi(x, \eta) \psi(u, \eta + \gamma) \psi(u, \gamma) d\eta d\gamma dx \quad (169)$$

$$= \int_0^{\infty} S(x, v) \int_{-\infty}^{\infty} \int_{-\infty}^{\infty} \Psi(x, t - s) \psi(u, t) \psi(u, s) dt ds dx, \quad (170)$$

where in (170) we made the substitutions $\eta \mapsto t - s$ and $\gamma \mapsto s$. Since

$$\Psi(x, t - s) = \int_{-\infty}^{\infty} \psi(x, r) \psi(x, r + t - s) dr = \int_{-\infty}^{\infty} \psi(x, y - t) \psi(x, y - s) dy, \quad (171)$$

where $r \mapsto y - t$, we have

$$\int_0^{\infty} S(x, v) A(u, x) dx = \int_{-\infty}^{\infty} \int_{-\infty}^{\infty} \int_0^{\infty} \int_{-\infty}^{\infty} S(x, v) \psi(x, y - t) \psi(x, y - s) \psi(u, t) \psi(u, s) dy dx dt ds \quad (172)$$

$$= \int_0^{\infty} \int_{-\infty}^{\infty} S(x, v) \left(\int_{-\infty}^{\infty} \psi(x, y - t) \psi(u, t) dt \right)^2 dy dx. \quad (173)$$

Using the fact that

$$|S(x, y + v) - S(x, v)| \leq 2MK(x) |y|, \quad (174)$$

as shown in the proof of Proposition 1, and following similar steps, we have

$$\left| \beta(u, v) - \int_0^{\infty} S(x, v) A(u, x) dx \right| \leq \left| 2M \int_0^{\infty} K(x) \int_{-\infty}^{\infty} |y| \left(\int_{-\infty}^{\infty} \psi(x, y + t) \psi(u, t) dt \right)^2 dy dx \right| \quad (175)$$

$$\leq \left| 2M\omega \int_0^{\infty} xK(x) \int_{-\infty}^{\infty} \left(\int_{-\infty}^{\infty} \psi(x, y + t) \psi(u, t) dt \right)^2 dy dx \right| \quad (176)$$

$$\leq \gamma \int_0^{\infty} xK(x) dx, \quad (177)$$

where again we set $\gamma = 2M\omega$. \square

Proof of Proposition 4

First of all, we have that

$$A(x, x) = \int_{-\infty}^{\infty} \Psi(x, \tau)^2 d\tau > 0. \quad (178)$$

Since A is continuous, we have that for each $x \in \mathbb{R}$, $A(x, y) > 0$ for all $y \in (x - g(x), x + g(x))$, for some function $g(x) > 0$. Now, assume that there exists $f \in N(T_A)$ such that $f \neq 0$. This means that

$$(T_A f)(x) = \int_0^{\infty} A(x, y) f(y) dy = 0, \quad \forall x \in \mathbb{R}^+. \quad (179)$$

Using the fact that $A(\beta x, \beta y) = \beta A(x, y)$ for all $\beta > 0$, we have

$$\int_0^{\infty} A(x, y) f(y) dy = \int_0^{\infty} xA\left(1, \frac{y}{x}\right) f(y) dy = \int_0^{\infty} x^2 A(1, u) f(xu) du, \quad (180)$$

where we used the substitution $y = xu$. Hence (179) becomes

$$\int_0^\infty A(1, u)f(xu) du = 0, \quad \forall x \in \mathbb{R}^+, \quad (181)$$

or equivalently

$$\langle A(1, \cdot), f(x \cdot) \rangle = 0 \quad \forall x \in \mathbb{R}^+, \quad (182)$$

which implies that $A(1, u) = 0$ for all $u \in \mathbb{R}^+$, a contradiction. Hence $N(T_A) = \{0\}$. \square

Proof of Theorem 2

Multiplying both sides of

$$c(t, \tau) = \int_0^\infty S(u, t)\Psi(u, \tau)du, \quad (183)$$

by $\Psi(u, \tau)$ and integrating, we have

$$\int_{-\infty}^\infty c(t, \tau)\Psi(u, \tau) d\tau = \int_0^\infty S(x, t)A(u, x) dx = (T_A S(\cdot, t))(u), \quad (184)$$

which, using the inverse of

$$(T_A f)(x) = \sum_{n=1}^\infty \lambda_n \langle \varphi_n, f \rangle \varphi_n(x), \quad (185)$$

we obtain

$$S(u, t) = \sum_{n=1}^\infty \frac{1}{\lambda_n} \varphi_n(u) \int_{-\infty}^\infty c(t, \tau) \langle \Psi(\cdot, \tau), \varphi_n \rangle d\tau \quad (186)$$

$$= \int_{-\infty}^\infty c(t, \tau) \sum_{n=1}^\infty \frac{1}{\lambda_n} \langle \Psi(\cdot, \tau), \varphi_n \rangle \varphi_n(u) d\tau, \quad (187)$$

as required. \square

Proof of Proposition 5

We have that

$$c_{X_T}(t, \tau) = \mathbb{E}[X_T(t)X_T(t + \tau)] \quad (188)$$

$$= \int_0^{J_\psi(T)} \int_{-\infty}^\infty |w_T(u, v)|^2 \psi(u, v - t) \psi(u, v - t - \tau) dv du \quad (189)$$

$$= \int_0^{J_\psi(T)} \int_{-\infty}^\infty |w_T(u, v + t)|^2 \psi(u, v) \psi(u, v - \tau) dv du, \quad (190)$$

where we used that $\mathbb{E}[L(du, dv)L(dx, dy)] = \delta(u - x)\delta(v - y) du dv dx dy$ and δ denotes the Dirac delta function. Now, from condition (c) in Definition 11, we have that

$$\left| w_T(u, v + t) - W\left(u, \frac{v + t}{T}\right) \right| \leq \frac{C(u)}{T}. \quad (191)$$

Furthermore, from the Lipschitz continuity of W , we also have that

$$\left| S\left(u, \frac{v + t}{T}\right) - S\left(u, \frac{t}{T}\right) \right| \leq 2MK(u) \left| \frac{v}{T} \right| \quad (192)$$

from which it follows that

$$\left| |w_T(u, v + t)|^2 - S\left(u, \frac{t}{T}\right) \right| \leq \frac{1}{T}(C(u) + 2MK(u)|v|). \quad (193)$$

Using the expression for $c(t, \tau)$ derived in the proof of Proposition 1 and replacing t with $z = t/T$, we have

$$|c_{X_T}(t, \tau) - c(z, \tau)| = \left| \int_0^{J_\psi(T)} \int_{-\infty}^{\infty} \left(|w_T(u, v+t)|^2 - S\left(u, \frac{t}{T}\right) \right) \psi(u, v) \psi(u, v-\tau) dv du \right| \quad (194)$$

$$\leq \left| \int_0^{J_\psi(T)} \int_{-\infty}^{\infty} \left| |w_T(u, v+t)|^2 - S\left(u, \frac{t}{T}\right) \right| \psi(u, v) \psi(u, v-\tau) dv du \right| \quad (195)$$

$$\leq \frac{1}{T} \left| \int_0^{J_\psi(T)} \int_{-\infty}^{\infty} (C(u) + 2MK(u)|v|) \psi(u, v) \psi(u, v-\tau) dv du \right| \quad (196)$$

$$\leq \frac{1}{T} \left| \int_0^{J_\psi(T)} (C(u) + \gamma u K(u)) \int_{-\infty}^{\infty} \psi(u, v) \psi(u, v-\tau) dv du \right| \quad (197)$$

$$= \frac{1}{T} \left| \int_0^{J_\psi(T)} (C(u) + \gamma u K(u)) \Psi(u, \tau) du \right| \quad (198)$$

$$\leq \frac{1}{T} \int_0^{J_\psi(T)} (C(u) + \gamma u K(u)) du \quad (199)$$

$$= O(T^{-1}), \quad (200)$$

since the integral is finite. \square

Proof of Theorem 3

We have that

$$\beta(u, z) = \beta\left(u, \frac{v}{T}\right) = \mathbb{E}[|d(u, v)|^2] = \mathbb{E}\left[\left(\int_{-\infty}^{\infty} X_T(t) \psi(u, t-v) dt\right)^2\right] \quad (201)$$

$$= \int_{-\infty}^{\infty} \int_{-\infty}^{\infty} \mathbb{E}[X_T(t) X_T(s)] \psi(u, t-v) \psi(u, s-v) dt ds \quad (202)$$

Now,

$$\mathbb{E}[X_T(t) X_T(s)] = \int_0^{J_\psi(T)} \int_{-\infty}^{\infty} |w_T(x, y)|^2 \psi(x, t-y) \psi(x, s-y) dx dy, \quad (203)$$

where we used that $\mathbb{E}[L(dx, dy) L(d\eta, d\xi)] = \delta(\eta-x) \delta(\xi-y) dx dy d\eta d\xi$ and δ is the Dirac delta function. Hence,

$$\beta(u, z) = \int_{-\infty}^{\infty} \int_{-\infty}^{\infty} \int_0^{J_\psi(T)} \int_{-\infty}^{\infty} |w_T(x, y)|^2 \psi(x, y-t) \psi(x, y-s) \psi(u, t-v) \psi(u, s-v) dy dx dt ds \quad (204)$$

$$= \int_{-\infty}^{\infty} \int_{-\infty}^{\infty} \int_0^{J_\psi(T)} \int_{-\infty}^{\infty} |w_T(x, y+v)|^2 \psi(x, y-t) \psi(x, y-s) \psi(u, t) \psi(u, s) dy dx dt ds \quad (205)$$

$$= \int_0^{J_\psi(T)} \int_{-\infty}^{\infty} |w_T(x, y+v)|^2 \left(\int_{-\infty}^{\infty} \psi(x, y-t) \psi(u, t) dt \right)^2 dy dx, \quad (206)$$

as in the proof of Theorem 1. From that proof we also have

$$\int_0^{J_\psi(T)} S(x, z) A(u, x) dx = \int_0^{J_\psi(T)} \int_{-\infty}^{\infty} S(x, z) \left(\int_{-\infty}^{\infty} \psi(x, y-t) \psi(u, t) dt \right)^2 dy dx, \quad (207)$$

where we have replaced v with its rescaled time counterpart z . Now, using the fact that

$$\left| |w_T(x, y+t)|^2 - S\left(x, \frac{t}{T}\right) \right| \leq \frac{1}{T} (C(x) + 2MK(x)|y|), \quad (208)$$

as shown in the proof of Proposition 5, we have

$$\begin{aligned} & \left| \beta(u, z) - \int_0^{J_\psi(T)} S(x, z) A(u, x) dx \right| \\ & \leq \frac{1}{T} \left| \int_0^{J_\psi(T)} \int_{-\infty}^{\infty} (C(x) + 2MK(x)|y|) \left(\int_{-\infty}^{\infty} \psi(x, y+t)\psi(u, t) dt \right)^2 dy dx \right| \end{aligned} \quad (209)$$

$$\leq \frac{1}{T} \left| \int_0^{J_\psi(T)} (C(x) + \gamma x K(x)) \int_{-\infty}^{\infty} \left(\int_{-\infty}^{\infty} \psi(x, y+t)\psi(u, t) dt \right)^2 dy dx \right| \quad (210)$$

$$\leq \frac{1}{T} \int_0^{J_\psi(T)} (C(x) + \gamma x K(x)) dx \quad (211)$$

$$= O(T^{-1}). \quad (212)$$

For the variance, we have that

$$\text{Var} [I(u, z)] = \mathbb{E} [I(u, z)^2] - \mathbb{E} [I(u, z)]^2 = 2\mathbb{E} [I(u, z)]^2. \quad (213)$$

This follows from

$$\mathbb{E} \left[\prod_{i=1}^4 L(du_i, dv_i) \right] = 3\delta(u_1 - u_2)\delta(v_1 - v_2)\delta(u_3 - u_4)\delta(v_3 - v_4) \prod_{i=1}^4 du_i dv_i, \quad (214)$$

since there are 3 ways to arrange the Lévy bases so that there are exactly 2 overlapping pairs, and so

$$\mathbb{E} [I(u, z)^2] = 3\mathbb{E} [I(u, z)]^2. \quad (215)$$

Therefore

$$\text{Var} [I(u, z)] = 2 \left[\int_0^{J_\psi(T)} A(u, x) S(x, z) dx + O(T^{-1}) \right]^2 \quad (216)$$

and so

$$\left| \text{Var} [I(u, z)] - 2 \left[\int_0^{J_\psi(T)} A(u, x) S(x, z) dx \right]^2 \right| = 2O(T^{-1}) \left[\int_0^{J_\psi(T)} A(u, x) S(x, z) dx + O(T^{-1}) \right] \quad (217)$$

$$= O(uT^{-1}), \quad (218)$$

since

$$\int_0^{J_\psi(T)} A(u, x) S(x, z) dx \leq A(u, u) \int_0^{J_\psi(T)} S(x, z) dx = \alpha u, \quad (219)$$

for some $\alpha \in \mathbb{R}^+$, as $A(u, u)$ is linear in u and $\int_0^\infty S(x, z) dx$ is finite by assumption. \square

Proof of Theorem 4

The proof is similar to that of [9]. We have that

$$\mathbb{E} \left(\tilde{d}_{\ell, m}^u \right) = \mathbb{E} \left[\int_0^1 I(u, z) \tilde{\psi}_{\ell, m}(z) dz \right] = \int_0^1 \beta(u, z) \tilde{\psi}_{\ell, m}(z) dz. \quad (220)$$

Now, using Theorem 3,

$$\left| \mathbb{E} \left(\tilde{d}_{\ell, m}^u \right) - \int_0^1 \int_0^\infty S(x, z) A(u, x) dx \tilde{\psi}_{\ell, m}(z) dz \right| \leq \left| \int_0^1 \frac{1}{T} \int_0^\infty (C(u) + \gamma u K(u)) du \tilde{\psi}_{\ell, m}(z) dz \right| \quad (221)$$

$$\leq \frac{1}{T} \int_0^\infty (C(u) + \gamma u K(u)) du \int_0^1 |\tilde{\psi}_{\ell, m}(z)| dz \quad (222)$$

$$= \frac{2^{\ell/2}}{T} \int_0^\infty (C(u) + \gamma u K(u)) du = O(2^{\ell/2} T^{-1}). \quad (223)$$

For the variance, is very similar to that of [9]. We substitute the spectrum f into equation (4.7) of Theorem 4.3 of [42] with the asymptotic limit $\int_0^\infty A(u, x) S(x, z) dx$. Since in our case u is fixed, we replace the two-dimensional wavelets with one-dimensional ones. Noting that $C_h = 1$ and N is proportional to u , where C_h and N are defined in [42], (80) follows from (ii) in the proof of Theorem 4.3 of [42], where the last term is exactly zero since we are assuming that the Lévy basis is Gaussian. This result is also similar to that of [43]. \square

Proof of Theorem 5

The proof closely follows the steps in [42] and [43]. It is easy to show that

$$\tilde{d}_{\ell,m}^u = X_T^T B_T X_T, \quad (224)$$

where superscript T denotes the transpose operation, $X_T = (X_T(t_0), \dots, X_T(t_{n(T)-1}))^T$ and B_T is an $n(T) \times n(T)$ matrix with entries

$$(B_T)_{i,j} = \frac{\tilde{\Delta}t_i \tilde{\Delta}t_j}{4M_v} \sum_{k=0}^{M_u-1} \psi(u, t_i - z_k T) \psi(u, t_j - z_k T) \tilde{\psi}_{\ell,m}(z_k). \quad (225)$$

Hence, we can get an equivalent expression for the wavelet coefficients $\tilde{d}_{\ell,m}^u$ to equation (4.11) of [42] and so Proposition 4.8 of [42] holds for $\tilde{d}_{\ell,m}^u$ as well. Therefore, as in [42],

$$\mathbb{P} \left(\left| \frac{\tilde{d}_{\ell,m}^u - d_{\ell,m}^u}{\tilde{\sigma}_{\ell,m}^u} \right| \geq \log(T) \right) = O \left(T^{-\frac{1}{2}} \right), \quad (226)$$

where $d_{\ell,m}^u$ denote the true wavelet coefficients of $\beta(u, \cdot)$. We note that

$$\text{Var} \left(\tilde{d}_{\ell,m}^u \right) = \int_0^1 \left[\int_0^\infty S(x, z) A(u, x) dx \right]^2 \tilde{\psi}_{\ell,m}^2(z) dz + O(2^\ell u T^{-2}) \quad (227)$$

$$= \int_0^1 \beta^2(u, z) \tilde{\psi}_{\ell,m}^2(z) dz + O(2^\ell u T^{-2}) \quad (228)$$

$$\leq 2T^{-1} \sup_{z \in (0,1)} \beta^2(u, z) \quad (229)$$

and therefore

$$\lambda(\ell, m, u, T) = \tilde{\sigma}_{\ell,m}^u \log(T) \leq \sqrt{2} \sup_{z \in (0,1)} |\beta(u, z)| T^{-\frac{1}{2}} \log(T). \quad (230)$$

Hence, the upper estimate of $\lambda(\ell, m, u, T)$ is equivalent to that of [42]. Since $\beta(u, \cdot)$ is Lipschitz continuous for each $u \in \mathbb{R}^+$, it is Holder continuous with $\sigma = 1$ (using the notation of [42]). Further, we are smoothing each level u separately and so the dimension in our setting is 1. Therefore (82) follows from a straightforward application of the results in Section 4.5 of [42]. \square

Proof of Proposition 8

We have that

$$\Psi(\tau) = \int_{-\infty}^{\infty} \psi(x) \psi(x - \tau) dx \quad (231)$$

$$= \int_{-\infty}^{\infty} \left(\mathbb{1}_{[0, \frac{1}{2}]}(x) - \mathbb{1}_{[\frac{1}{2}, 1]}(x) \right) \left(\mathbb{1}_{[0, \frac{1}{2}]}(x - \tau) - \mathbb{1}_{[\frac{1}{2}, 1]}(x - \tau) \right) dx \quad (232)$$

$$= \int_{-\infty}^{\infty} \left(\mathbb{1}_{[0, \frac{1}{2}]}(x) - \mathbb{1}_{[\frac{1}{2}, 1]}(x) \right) \left(\mathbb{1}_{[\tau, \frac{1}{2} + \tau]}(x) - \mathbb{1}_{[\frac{1}{2} + \tau, 1 + \tau]}(x) \right) dx \quad (233)$$

$$= \int_{-\infty}^{\infty} \mathbb{1}_{[0, \frac{1}{2}] \cap [\tau, \frac{1}{2} + \tau]}(x) - \mathbb{1}_{[\frac{1}{2}, 1] \cap [\tau, \frac{1}{2} + \tau]}(x) - \mathbb{1}_{[0, \frac{1}{2}] \cap [\frac{1}{2} + \tau, 1 + \tau]}(x) + \mathbb{1}_{[\frac{1}{2}, 1] \cap [\frac{1}{2} + \tau, 1 + \tau]}(x) dx \quad (234)$$

$$= 2 \left(\frac{1}{2} - |\tau| \right) \mathbb{1}_{[-\frac{1}{2}, \frac{1}{2}]}(\tau) - \left(\frac{1}{2} - \left| \tau - \frac{1}{2} \right| \right) \mathbb{1}_{[0, 1]}(\tau) - \left(\frac{1}{2} - \left| \tau + \frac{1}{2} \right| \right) \mathbb{1}_{[-1, 0]}(\tau) \quad (235)$$

$$= \begin{cases} 1 - 3|\tau|, & 0 < |\tau| \leq 1/2, \\ |\tau| - 1, & 1/2 < |\tau| \leq 1, \\ 0, & \text{otherwise.} \end{cases} \quad (236)$$

Using property (iii) from Proposition 2, we have

$$\Psi(u, \tau) = \begin{cases} 1 - 3|\tau|/u, & 0 < |\tau| \leq u/2, \\ |\tau|/u - 1, & u/2 < |\tau| \leq u, \\ 0, & \text{otherwise,} \end{cases} \quad (237)$$

as required. \square

Proof of Proposition 9

We have

$$A(u, x) = \int_{-\infty}^{\infty} \Psi(u, y) \Psi(x, y) dy \quad (238)$$

$$= \int_{-\infty}^{\infty} \left(\left(1 - 3 \frac{|y|}{u} \right) \mathbb{1}_{[0, \frac{u}{2}]}(|y|) + \left(\frac{|y|}{u} - 1 \right) \mathbb{1}_{[\frac{u}{2}, u]}(|y|) \right) \left(\left(1 - 3 \frac{|y|}{x} \right) \mathbb{1}_{[0, \frac{x}{2}]}(|y|) + \left(\frac{|y|}{x} - 1 \right) \mathbb{1}_{[\frac{x}{2}, x]}(|y|) \right) dy \quad (239)$$

The result is easily obtained by evaluating each of the cross terms individually. \square

Proof of Proposition 10

We have that

$$\Psi(u, \tau) = \int_{-\infty}^{\infty} \psi(u, x) \psi(u, x - \tau) dx \quad (240)$$

$$= \frac{4}{3u\sqrt{\pi}} \int_{-\infty}^{\infty} \left(1 - \frac{x^2}{u^2} \right) \left(1 - \frac{(x - \tau)^2}{u^2} \right) \exp \left\{ -\frac{x^2 + (x - \tau)^2}{2u^2} \right\} dx \quad (241)$$

$$= \frac{4}{3u\sqrt{\pi}} \int_{-\infty}^{\infty} \left(1 - \frac{x^2 + (x - \tau)^2}{u^2} + \frac{x^2(x - \tau)^2}{u^4} \right) \exp \left\{ -\frac{(x - \frac{\tau}{2})^2 + \frac{\tau^2}{4}}{u^2} \right\} dx \quad (242)$$

$$= \frac{4e^{-\frac{\tau^2}{4u^2}}}{3u\sqrt{\pi}} \int_{-\infty}^{\infty} \left(1 - 2\frac{(x - \frac{\tau}{2})^2 + \frac{\tau^2}{4}}{u^2} + \frac{x^2(x - \tau)^2}{u^4} \right) \exp \left\{ -\frac{(x - \frac{\tau}{2})^2}{u^2} \right\} dx, \quad (243)$$

where we completed the square in the exponential. Now, using the transform

$$y = \sqrt{2} \frac{x - \tau/2}{u}, \quad (244)$$

we have

$$\Psi(u, \tau) = \frac{4}{3} e^{-\frac{\tau^2}{4u^2}} \int_{-\infty}^{\infty} \left(1 - \frac{\tau^2}{2u^2} + \frac{\tau^4}{16u^4} - \left(1 + \frac{\tau^2}{4u^2} \right) y^2 + \frac{1}{4} y^4 \right) \frac{1}{2\sqrt{\pi}} e^{-\frac{y^2}{2}} dy \quad (245)$$

$$= \frac{4}{3} e^{-\frac{\tau^2}{4u^2}} \left(1 - \frac{\tau^2}{2u^2} + \frac{\tau^4}{16u^4} - \left(1 + \frac{\tau^2}{4u^2} \right) + \frac{3}{4} \right) \quad (246)$$

$$= \left(1 + \frac{\tau^4}{12u^4} - \frac{\tau^2}{u^2} \right) e^{-\frac{\tau^2}{4u^2}}, \quad (247)$$

where we used the fact that we are integrating against the probability density function of a standard normal distribution and so can use its moments. \square

Proof of Proposition 11

We have

$$A(u, x) = \int_{-\infty}^{\infty} \Psi(u, y) \Psi(x, y) dy \quad (248)$$

$$= \int_{-\infty}^{\infty} \left(1 + \frac{\tau^4}{12u^4} - \frac{\tau^2}{u^2} \right) \left(1 + \frac{\tau^4}{12x^4} - \frac{\tau^2}{x^2} \right) \exp \left\{ -\frac{\tau^2}{4u^2} - \frac{\tau^2}{4x^2} \right\} d\tau \quad (249)$$

$$= \int_{-\infty}^{\infty} \left(1 - \left(\frac{1}{x^2} + \frac{1}{u^2} \right) \tau^2 + \left(\frac{1}{12u^4} + \frac{1}{x^2u^2} + \frac{1}{12x^4} \right) \tau^4 - \frac{1}{12} \left(\frac{1}{u^2x^4} + \frac{1}{u^4x^2} \right) \tau^6 + \frac{1}{144u^4x^4} \tau^8 \right) \exp \left\{ -\frac{1}{4} \left(\frac{1}{u^4} + \frac{1}{x^4} \right) \tau^2 \right\} d\tau. \quad (250)$$

Setting

$$y^2 = \frac{1}{2} \left(\frac{1}{u^2} + \frac{1}{x^2} \right) \tau^2, \quad (251)$$

we have

$$A(u, x) = 2\sqrt{\frac{\pi u^2 x^2}{u^2 + x^2}} \int_{-\infty}^{\infty} \left(1 - 2y^2 + \frac{1}{3}y^4 + \frac{10u^2 x^2}{3(u^2 + x^2)^2} y^4 - \frac{2u^2 x^2}{3(u^2 + x^2)^2} y^6 + \frac{u^4 x^4}{9(u^2 + x^2)^4} y^8 \right) \frac{1}{2\pi} e^{-\frac{y^2}{2}} dy \quad (252)$$

$$= 2\sqrt{\frac{\pi u^2 x^2}{u^2 + x^2}} \left(1 - 2 + 1 + \frac{10u^2 x^2}{(u^2 + x^2)^2} - \frac{10u^2 x^2}{(u^2 + x^2)^2} + \frac{35u^4 x^4}{3(u^2 + x^2)^4} \right) \quad (253)$$

$$= \frac{70\sqrt{\pi}}{3} \frac{u^5 x^5}{(u^2 + x^2)^{\frac{9}{2}}}, \quad (254)$$

where again we used the fact that we are integrating against the probability density function of a standard normal. \square

Proof of Proposition 12

To begin with, we have that

$$\Psi(u, \tau) = \int_{-\infty}^{\infty} \psi(u, x)\psi(u, x - \tau)dx = \int_{-\infty}^{\infty} \psi(u, x)\psi(u, \tau - x)dx = \psi(u, \cdot) * \psi(u, \cdot) \quad (255)$$

as Shannon wavelets are symmetric and where $*$ denotes the convolution operator. Hence

$$\hat{\Psi}(u, \omega) = \hat{\psi}(u, \omega)\hat{\psi}(u, \omega) = \sqrt{u} \hat{\psi}(u, \omega), \quad (256)$$

since the square of an indicator function is simply equal to the indicator function and the cross term is zero since the intervals are non-overlapping. Hence, taking the inverse Fourier transform

$$\Psi(u, \tau) = \sqrt{u} \psi(u, \tau), \quad (257)$$

as required. \square

Proof of Proposition 13

We have

$$A(u, x) = \int_{-\infty}^{\infty} \Psi(u, y)\Psi(x, y) dy \quad (258)$$

$$= \sqrt{ux} \int_{-\infty}^{\infty} \psi(u, y)\psi(x, y) dy \quad (259)$$

$$= \sqrt{ux} \int_{-\infty}^{\infty} \psi(u, y)\psi(x, -y) dy \quad (260)$$

$$= \sqrt{ux} \mathcal{F}^{-1}(\hat{\psi}(u, \cdot)\hat{\psi}(x, \cdot))(0) \quad (261)$$

where we used the convolution theorem and $\mathcal{F}^{-1}(f)(0)$ denotes the inverse Fourier transform of the function f evaluated at zero. Now, for $x > 2u$, the above is clearly zero as none of the intervals in the indicator functions overlap. For $u \leq x \leq 2u$, we have

$$\hat{\psi}(u, \omega)\hat{\psi}(x, \omega) = \sqrt{ux} \left(\mathbb{1}_{[-\frac{2\pi}{x}, -\frac{\pi}{u}]}(\omega) + \mathbb{1}_{[\frac{\pi}{u}, \frac{2\pi}{x}]}(\omega) \right) \quad (262)$$

The case $x < u$ is symmetrical. Taking the inverse Fourier transform of the above, we obtain

$$\mathcal{F}^{-1}(\hat{\psi}(u, \cdot)\hat{\psi}(x, \cdot))(y) = \frac{\sqrt{ux}}{2\pi} \int_{-\frac{2\pi}{x}}^{-\frac{\pi}{u}} e^{i2\pi\omega y} d\omega + \frac{1}{2\pi} \int_{\frac{\pi}{u}}^{\frac{2\pi}{x}} e^{i2\pi\omega y} d\omega \quad (263)$$

$$= \frac{\sqrt{ux}}{i4\pi^2 y} \left(e^{i4\pi^2 \frac{y}{x}} - e^{i2\pi^2 \frac{y}{u}} + e^{-i2\pi^2 \frac{y}{u}} + e^{-i4\pi^2 \frac{y}{x}} \right) \quad (264)$$

$$= \frac{\sqrt{ux}}{2\pi^2 y} \left(\sin\left(\frac{4\pi^2 y}{x}\right) - \sin\left(\frac{2\pi^2 y}{x}\right) \right) \quad (265)$$

Now,

$$\frac{\sqrt{ux}}{2\pi^2 y} \left(\sin\left(\frac{4\pi^2 y}{x}\right) - \sin\left(\frac{2\pi^2 y}{x}\right) \right) \rightarrow \sqrt{ux} \left(\frac{2}{x} - \frac{1}{u} \right), \quad \text{as } y \rightarrow 0, \quad (266)$$

since

$$\lim_{y \rightarrow 0} \frac{\sin(\alpha y)}{y} = \alpha. \quad (267)$$

Hence, we have $A(u, x) = 2u - x$, $u \leq x \leq 2u$ and the rest follows by symmetry. \square